TURUN YLIOPISTON JULKAISUJA
ANNALES UNIVERSITATIS TURKUENSIS

SARJA - SER. D OSA - TOM. 1096

MEDICA - ODONTOLOGICA

DIFFUSION TENSOR IMAGING AS A DIAGNOSTIC AND RESEARCH TOOL: A STUDY ON PRETERM INFANTS

by

Virva Saunavaara

née Lepomäki

TURUN YLIOPISTO
UNIVERSITY OF TURKU
Turku 2013

From Department of Cell Biology and Anatomy (Laboratory of Biophysics), Institute of Biomedicine, the Department of Radiology, the Institute of Clinical Medicine, and the Turku PET Center, Faculty of Medicine and Turku Doctoral Program of Clinical Sciences, and International Doctoral Program in Biomedical Engineering and Medical Physics, University of Turku, Turku, Finland

Supervised by
Professor Riitta Parkkola
Department of Radiology
University of Tampere
Tampere, Finland

PhD Markku Komu
Department of Radiology
University of Turku
Turku, Finland

Reviewed by
Docent Outi Sipilä
Department of Physics, University of Helsinki
Helsinki Medical Imaging Center, Helsinki University Central Hospital
Helsinki, Finland

Docent Leena Valanne
Department of Radiology
Helsinki University Central Hospital
Helsinki, Finland

Opponent
Professor Miika Nieminen
Department of Radiology
University of Oulu and Oulu University Central Hospital
Oulu, Finland

ISBN 978-951-29-5595-4 (PRINT)
ISBN 978-951-29-5596-1 (PDF)
ISSN 0355-9483
Painosalama Oy – Turku, Finland 2013

Täyttyneen toiveen tilalle astuu aina uusi
Arthur Schopenhauer

ABSTRACT

Virva Saunavaara
DIFFUSION TENSOR IMAGING AS A DIAGNOSTIC AND RESEARCH TOOL: A STUDY ON PRETERM INFANTS

From Department of Cell Biology and Anatomy
University of Turku, Turku Finland
Annales Universitatis Turkuensis SER. D TOM. 1096, Painosalama Oy - Turku, Finland 2013

Diffusion tensor imaging (DTI) is an advanced magnetic resonance imaging (MRI) technique. DTI is based on free thermal motion (diffusion) of water molecules. The properties of diffusion can be represented using parameters such as fractional anisotropy, mean diffusivity, axial diffusivity, and radial diffusivity, which are calculated from DTI data. These parameters can be used to study the microstructure in fibrous structure such as brain white matter.

The aim of this study was to investigate the reproducibility of region-of-interest (ROI) analysis and determine associations between white matter integrity and antenatal and early postnatal growth at term age using DTI. Antenatal growth was studied using both the ROI and tract-based spatial statistics (TBSS) method and postnatal growth using only the TBSS method.

The infants included to this study were born below 32 gestational weeks or birth weight less than 1,501 g and imaged with a 1.5 T MRI system at term age. Total number of 132 infants met the inclusion criteria between June 2004 and December 2006. Due to exclusion criteria, a total of 76 preterm infants (ROI) and 36 preterm infants (TBSS) were accepted to this study.

The ROI analysis was quite reproducible at term age. Reproducibility varied between white matter structures and diffusion parameters.

Normal antenatal growth was positively associated with white matter maturation at term age. The ROI analysis showed associations only in the corpus callosum. Whereas, TBSS revealed associations in several brain white matter areas. Infants with normal antenatal growth showed more mature white matter compared to small for gestational age infants. The gestational age at birth had no significant association with white matter maturation at term age.

It was observed that good early postnatal growth associated negatively with white matter maturation at term age. Growth-restricted infants seemed to have delayed brain maturation that was not fully compensated at term, despite catch-up growth.

Key words: magnetic resonance imaging, diffusion tensor imaging, preterm infant

TIIVISTELMÄ

Virva Saunavaara
DIFFUUSIOTENSORIKUVAUS DIAGNOSTISENA JA TUTKIMUSTYÖKALUNA KESKOSTUTKIMUKSESSA

Solubiologian ja anatomian oppiaine
Turun Yliopisto, Turku Suomi
Annales Universitatis Turkuensis SER. D TOM. 1096, Painosalama Oy - Turku, Suomi 2013

Diffuusiotensorikuvaus (DTI) on magneettikuvauksen erikoistekniikka. DTI perustuu veden vapaaseen lämpöliikkeeseen (diffuusioon). Diffuusion ominaisuuksia voidaan esittää DTI-datasta laskettavien parametrien avulla. Tällaisia parametreja ovat esimerkiksi fraktionaalinen anisotropia, keskimääräinen diffusiviteetti, aksiaalinen ja radiaalinen diffusiviteetti. Näitä parametrejä voidaan käyttää säikeisten rakenteiden esimerkiksi aivojen valkoisen aineen tutkimiseen.

Tässä tutkimuksessa selvitettiin keskosten aivojen diffuusiotensorikuvista tehtyjen mielenkiintoalueisiin (ROI) perustuvien mittausten toistettavuutta sekä tutkittiin valkoisen aineen kypsyyden ja raskauden aikaisen sekä varhaisen postnataalisen kasvun välistä yhteyttä. Raskauden aikaisen kasvun vaikutusta tutkittiin käyttäen sekä ROI- että TBSS-tekniikoita. Postnataalista kasvua tarkasteltiin ainoastaan TBSS-tekniikalla.

Tähän tutkimukseen otettiin mukaan keskoset, jotka syntyivät ennen 32 raskausviikkoa tai joiden syntymäpaino oli alle 1,501 g sekä MRI kuvaus oli tehty lasketunajan kohdalla. Tutkimukseen hyväksyttiin kesäkuun 2004 ja joulukuun 2006 välillä 132 keskosta. Poissulkukriteerien takia 76 keskosta (ROI) ja 36 (TBSS) hyväksyttiin tähän tutkimukseen.

ROI-analyysi osoittautui melko toistettavaksi lasketun ajan iässä. Toistettavuus vaihteli sekä valkoisen aineen rakenteiden että diffuusioparametrien välillä.

Normaali raskauden aikainen kasvu liittyi hyvään valkoisen aineen kehitykseen lasketunajan kohdalla. ROI-tekniikalla yhteys havaittiin corpus callosumin alueella. TBSS-menetelmä puolestaan näytti yhteyden usealla eri valkoisen aineen alueella. Syntymähetken gestaatioiällä ei havaittu yhteyttä valkoisen aineen kehitysasteeseen lasketun ajan kohdalla.

Hyvän varhaisen vaiheen postnataalisen kasvun havaittiin liittyvän heikompaan valkoisen aineen kehitysasteeseen lasketunajan kohdalla. Saavutuskasvu ei ollut korjannut raskauden aikaisen kasvuhäiriön vaikutusta aivojen kypsyyteen laskettuun aikaan mennessä.

Avainsanat: magneettikuvaus, diffuusiotensorikuvaus, keskonen

CONTENTS

ABBREVIATIONS

AAL	automated anatomical labeling
AD	axial diffusivity
AGA	appropriate for gestational age
CC	corpus callosum
COLL	colliculus inferior
CP	cerebral palsy
CR	corona radiata
CSF	cerebrospinal fluid
CT	computed tomography
DEC	directionally encoded color
DTI	diffusion tensor imaging
DW	diffusion weighted
DWI	diffusion weighted imaging
ELWB	extremely low birth weight
EPI	echo-planar imaging
FA	fractional anisotropy
FDT	FMRIB's Diffusion Toolbox
FID	free induction decay
FLAIR	Fluid-Attenuated Inversion Recovery
FSL	FMRIB (Functional MRI of Brain) Software Library
FWE	Free Water Elimination
GA	gestational age
GM	grey matter
HC	head circumference
IC	internal capsule
ICC	intraclass correlation coefficient
IUGR	intrauterine growth restriction
JHU	John Hopkins University
MD	mean diffusivity
MR	magnetic resonance
MRI	magnetic resonance imaging
Mxy	transverse magnetization
Mz	net magnetization
NMR	nuclear magnetic resonance
OR	optic radiation
PLIC	posterior limb of the internal capsule
PVE	partial volume effect
RD	radial diffusivity
RF	radio frequency
ROI	region-of-interest

SD	standard deviations
SE-EPI	spin echo echo-planar imaging
SGA	small for gestational age
SNR	signal-to-noise ratio
SPIR	Spectral Presaturation with Inversion Recovery
SPM	Statistical Parametric Mapping
T1	spin–lattice (longitudinal) relaxation time
T2	spin–spin (transverse) relaxation time
T2*	transverse relaxation time when combining magnetic field inhomogeneities and spin-spin relaxation
TBSS	tract-based-spatial-statistic
TE	echo time
TFCE	threshold-free cluster enhancement
TI	inversion time
TR	repetition time
TSE	turbo spin echo
VBM	voxel-based morphometry
VLBW	very low birth weight
WHO	World Health Organization
WM	white matter
RMS	root mean square displacement
VLGA	very low gestational age

LIST OF ORIGINAL PUBLICATIONS

This thesis is based on the following publications:

I. Fractional anisotropy and mean diffusivity parameters of the brain white matter tracts in preterm infants: reproducibility of region-of-interest measurements. Lepomäki Virva, Paavilainen Teemu, Hurme Saija, Komu Markku, and Parkkola Riitta. *Pediatric Radiology* 2012; 42(2):175-82.

II. Effect of antenatal growth and prematurity on brain white matter: diffusion tensor study. Lepomäki Virva, Paavilainen Teemu, Matomäki Jaakko, Hurme Saija, Haataja Leena, Lapinleimu Helena, Lehtonen Liisa, Komu Markku, and Parkkola Riitta. *Pediatric Radiology* 2012; 42(6):692-8.

III. Effect of antenatal growth on brain white matter maturation in preterm infants at term using tract-based spatial statistics. Lepomäki Virva, Matomäki Jaakko, Lapinleimu Helena, Lehtonen Liisa, Haataja Leena, Komu Markku, and Parkkola Riitta. *Pediatric Radiology* 2013; 43(1): 80-5.

IV. Preterm infants' early growth and brain white matter maturation at term age. Lepomäki Virva, Leppänen Marika, Matomäki Jaakko, Lapinleimu Helena, Lehtonen Liisa, Haataja Leena, Komu Markku, Rautava Päivi, and Parkkola Riitta. *Pediatric Radiology* 2013; 43(10):1357-1364

The publications are referred to in the text by their roman numerals. The original publications have been reprinted with the permission of the copyright holders.

1 INTRODUCTION

Magnetic resonance imaging has several advantages compared to other imaging modalities: it is non-invasive and uses non-ionizing radiation. One of the major advantages is the excellent soft-tissue contrast. The phenomenon of nuclear magnetic resonance (NMR) was independently discovered in 1946 by Felix Bloch and Edward Purcell (Bloch 1946, Purcell et al. 1946). They were awarded the 1952 Nobel Prize in Physics. In 1971, Raymond Damadian reported that relaxation times of the NMR signal in tumors were significantly different from normal tissue in vitro (Damadian 1971). The excellent contrast difference between diseased and normal tissue is the strength of magnetic resonance imaging (MRI) even today. Spatial localization of the NMR signal using magnetic field gradients was implemented separately by Paul Lauterbur (Lauterbur 1973) and Peter Mansfield (Garroway et al. 1974, Mansfield et al. 1973). They were jointly awarded the 2003 Nobel Prize in Physiology or Medicine. This was the starting point of medical imaging using MRI and since then it has become the fastest-growing imaging method. For example, in Finland the first MRI scanner was installed in 1984. By 1996 the number of scanners had increased to 31 and by 2005 to 75. In that same period, the number of computed tomography (CT) scanners increased from 60 to 80. Despite their relatively high price, there are around 120 MRI scanners in Finland today (2013) (STUK 2013).

MRI is a very versatile imaging modality. A typical MRI study consists of several sequences that produce various image contrasts, such as T1, T2, T2*, and proton density weighted images which are mostly applied in basic anatomical imaging. Sometimes contrast can be even further enhanced using gadolinium-based contrast agents. In addition, more advanced sequences can be used to visualize blood vessels (magnetic resonance angiography), or to measure brain activations (functional MRI, fMRI).

Diffusion tensor imaging (DTI) is one of these more advanced MRI techniques. DTI can bring additional value to conventional MRI, as it provides knowledge about tissue microstructure (Le Bihan et al. 2001). DTI can be used to describe the microstructure in fibrous structure (for example brain white matter) as water molecules tend to diffuse along fiber bundles (Van Kooij et al. 2012). This can be extremely important in infants, as DTI makes it possible to study the maturation of white matter prior to conventional anatomical MRI. The history of diffusion tensor imaging started with the discovery of random thermal motion, also known as Brownian motion. The discovery was made by Robert Brown in the early 1800s (Brown 1827). The mathematical basis for diffusion was formed by Henri Hureau de Sénarmont, Adolf Eugen Fick, and Albert Einstein, among others. Edward Stejskal and John Tanner made the important finding regarding imaging sequences: they used two pulsed gradients to measure diffusion in NMR experiments (Stejskal et al. 1965). Peter Mansfield introduced the principles of the echo-planar imaging (EPI) technique (Mansfield 1977) that is still the basis of most typical DTI sequences. In 1994,

Basser and LeBihan published the mathematical basis for tensor-based diffusion anisotropy imaging (Basser et al. 1994b).

The present work investigated the usability of DTI in assessing the white matter maturation of preterm infants imaged at term age. Perinatal mortality in Finland is one of the lowest in the world, and even smaller preterm infants survive. In 2010 the perinatal mortality rate was 4 infants per thousand live births. However, preterm birth is considered as a risk for normal brain development. In 2010, a total of 61,191 infant were born alive. A 5.8 percentage were born premature (gestational age less than 37 weeks). The vulnerability of the brain is dependent on the developmental stage. In addition to premature birth, the birth weight and catch-up growth are also associated with brain maturation and the future outcome of the infants. The associations between antenatal- and early postnatal growth and diffusion parameters that reflect white matter maturation were studied. The clinical analysis method used in this work was region-of-interest (ROI) analysis and the research method was the tract-based-spatial-statistic (TBSS). We also assessed the intra- and inter reproducibility of the ROI method.

2 REVIEW OF LITERATURE

2.1 DIFFUSION TENSOR IMAGING

2.1.1 MAGNETIC RESONANCE IMAGING

Magnetic resonance imaging is usually based on the physical properties of the hydrogen nucleus (^{1}H). All nuclei have an intrinsic property called spin. The spin of proton, the nucleus of hydrogen atom, is ½ (Dixon et al. 1982). Nuclei with nonzero spin possess intrinsic nuclear magnetism called magnetic moment (Levitt 2001). Therefore magnetic moment is observed also in several other nuclei in nature such as phosphorus (^{31}P) and sodium (^{23}Na), and those nuclei can also be observed with MRI. However, their gyromagnetic ratio (a magnetic property of the nucleus) is lower than the one of hydrogen (Levitt 2001). In addition they are much less abundant than hydrogen in biological tissues. As a result the intensity of the observable signal is only a fraction of that of hydrogen.

In an external magnetic field B_0, a small excess of magnetic moments are biased towards the direction of the external magnetic field and therefore a net magnetization (Mz) is formed (Hahn 1950). In MRI related literature magnetic moments are often referred as spins. As a result of the external field, the spins (i.e. magnetic moment) also perform a process called precession. The precession frequency f_0, called the Larmor frequency, depends on the nucleus and is proportional to the strength of the applied magnetic field

$$f_0 = \frac{\gamma}{2\pi} B_0 \ ,$$

where γ is the gyromagnetic ratio (Mansfield et al. 1978). Protons have a gyromagnetic ratio of γ = 42.58 MHz/T, resulting in a Larmor frequency of 63.9 MHz at 1.5 T. However, there is no phase coherence between the spins.

The absorption of electromagnetic energy by atomic nuclei is called excitation. The MR signal is created using an electromagnetic wave, an radio frequency (RF) pulse, at the resonance frequency (Hahn 1950). The amplitude and duration of the RF pulse determine the overall energy transfer. RF pulse rotates the net magnetization vector to transverse plane. This is referred as transverse magnetization (Mxy). This transverse magnetization can be measured using an RF coil. Following the excitation, the spins will have spin-lattice and spin-spin interactions (Bloch 1946). These are more commonly referred to as the relaxation processes. The spin-lattice and spin-spin relaxation processes are better known as T1 relaxation and T2 relaxation, respectively. T1 relaxation describes the rate of the magnetization recovery in z-direction. T2 relaxation, in turn, describes the rate of decreasing magnetization in transverse plane. T1 and T2 are tissue-related parameters.

In a basic MRI experiment, two RF pulses (excitation and refocusing RF pulses) are applied and the observed signal is known as the spin echo. An echo signal can also result from the use of gradient reversal on the frequency-encoded axis: it is then referred to as a gradient echo. These echoes are normally referred to as the MR signal. Differences in relaxation times between tissues are utilized to form different contrasts in MR images (Mansfield et al. 1978). This is done, for example, by changing the timing (echo time, TE), order, and repetition frequency of the RF pulses.

Magnetic field gradients are used to encode location information into the MR signal (Lauterbur 1973). Magnetic field gradients are magnetic fields which alter the magnetic field strength along the chosen direction. The gradients are activated at specific time points during imaging, for example during the RF pulse, to produce selective slice excitation, phase encoding, and frequency encoding.

Echo signals are usually collected row by row into a data matrix known as k-space. However, there are other sampling techniques as well. In a simple experiment one row is collected after each excitation. The time between excitation pulses is known as repetition time (TR). The final image is formed using 2D- or 3D inverse Fourier transform (Bernstein et al. 2004).

2.1.2 PHYSICAL BASIS OF DTI

2.1.2.1 Diffusion

Diffusion is free thermal motion of molecules, also known as Brownian motion. In isotropic diffusion, the motion of the water molecules is independent of the direction. The behavior of unrestricted diffusion is described by Einstein's equation

$$\sigma = \sqrt{2Dt},$$

where σ is the average diffusion distance, D is the diffusion coefficient, and t is the diffusion time.

Obstacles can hinder diffusion and the restrictions can be greater in one direction than in others (Beaulieu 2002). This causes a property of diffusion known as anisotropy. In biological tissue, diffusion of water molecules is hindered by the presence of macromolecules, organelles, cell membranes, and other cellular and subcellular structures (Le Bihan 1995). Therefore, water diffusion does not usually have spherical symmetry in biological tissue. Diffusion anisotropy provides quantitative knowledge about the tissue microstructure (Le Bihan et al. 2001)

2.1.2.2 Single-shot SE-EPI

The most used sequence for DTI is single-shot spin-echo echo-planar imaging (SE-EPI). SE-EPI has the advantage of freezing bulk motion. However, the spatial resolution is low compared to the normal anatomical MR resolution, its typical resolution being 2-3 mm.

SE-EPI is an ultrafast imaging sequence, as each 2D image is gathered after a single excitation (Mansfield 1977, Stehling et al. 1991). SE-EPI uses two RF pulses, one excitation pulse with a flip angle of 90 and a refocusing pulse with a flip angle of 180. Fat suppression is necessary in SE-EPI, and this can be achieved, for example, using a spectral presaturation with inversion-recovery (SPIR) (Bernstein et al. 2004). SE-EPI relies on gradient echoes to sample k-space lines. However, the gradient echoes are formed under the spin echo envelope instead of an FID (Bernstein et al. 2004). Each gradient echo is acquired at a different echo time (TE). The effective TE of the sequence is defined as the TE when the central k-space line is acquired. The image becomes predominantly T2 weighted if the effective TE is as long or longer as T2 relaxation time and assuming that repetition time (TR) is larger than T1 relaxation time (Bernstein et al. 2004).

Diffusion weighted images are acquired by adding diffusion weighting gradients to SE-EPI sequences as seen in Figure 1. (Le Bihan et al. 2006). Diffusion weighting gradients are placed on both sides of the 180° refocusing pulse (Bammer et al. 2002, Stejskal et al. 1965). Diffusion of water molecules causes a phase dispersion of the transverse magnetization, which results in attenuation of the MR signal. The amount of signal loss is characterized by the tissue structure, and physical and physiological state as well as the microenvironment. Assuming Gaussian diffusion, the signal strength in the diffusion weighted image when using pair of balanced diffusion-sensitizing gradient can be expressed using Stejskal-Tanner equation

$$I = I_0 e^{-bD}$$

where I_0 is the signal strength without diffusion gradients and the b-value is

$$b = \gamma^2 G^2 \delta^2 \left(\Delta - \frac{\delta}{3}\right),$$

where γ is the gyromagnetic ratio, G is the strength of diffusion encoding gradients, δ is the gradient duration, and Δ is the gradient separation for the pulsed gradient spin-echo experiment (Bernstein et al. 2004). The selection of the optimal b-value can be challenging. If the b value is too low, the signal attenuation cannot be measured. On the other hand, if the b value is too high, the signal would decay to noise level. In practice, a b range from 600 to 1200 s/mm² is used for clinical DTI studies. In addition to diffusion weighted images, also image without diffusion weighting is needed (b_0-image).

Imaging artifacts are caused by the used pulse sequence. Therefore, EPI-based DTI sequences inherit all of the artifacts of EPI. Typical artifacts include T2/T2* blurring, Nyquist ghosts and chemical shift artifacts, susceptibility artifacts, and eddy currents. Parallel imaging techniques, such as sensitivity encoding (SENSE), can be used to reduce image distortion and blurring artifacts in DTI-EPI (Bammer et al. 2002). However, use of the parallel imaging technique causes a lower signal-to-noise ratio (SNR) (Pruessmann et al. 1999). This can be problematic for DTI studies (Basser et al. 2000a). Eddy currents can be reduced using the twice refocused spin echo EPI imaging technique (Reese et al. 2003).

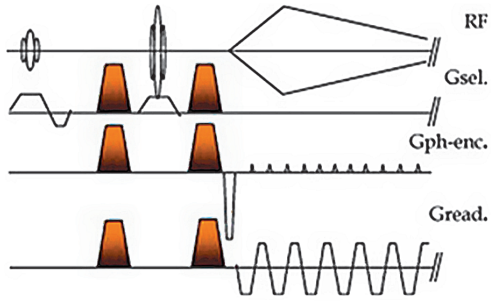

Figure 1. Diffusion-weighted spin-echo EPI sequence. Reprinted with permission from the copyright holder (Copyright © 2006 Wiley-Liss, Inc).

2.1.2.3 Diffusion tensor

Diffusion tensor imaging was developed in the early 1990s (Basser et al. 1994b, Pierpaoli et al. 1996b). In diffusion tensor imaging, the diffusion weighted imaging (DWI) images must be collected in at least 6 non-collinear directions. In addition, b_0-image image is needed. However, in practice, 32 or more directions are often used. The tensor model is fitted to the measured diffusion weighted data (Basser et al. 1994a). Basically, the diffusion tensor is a symmetrical 3 x 3 matrix. A set of eigenvalues ($\lambda 1$, $\lambda 2$, $\lambda 3$) and eigenvectors ($v1$, $v2$, $v3$) can be determined from the diffusion tensor. The diffusion tensor can be visualized using the diffusion ellipsoid, as shown in Figure 2. The $\lambda 1$ direction is often referred to as the principal diffusion direction.

The parametric images that characterize the properties of diffusion can be determined from the eigenvalues (such as fractional anisotropy (FA) and mean diffusivity (MD) images). Directionally encoded color (DEC) maps can also be determined using the eigenvectors (Pajevic et al. 1999). Rotationally invariant parameters should be preferred, as they are independent of the tissue's orientation in the laboratory frame of reference, unlike parameters calculated from three perpendicular gradient directions (Papadakis et al. 1999, Pierpaoli et

al. 1996a). Rotationally invariant parameters include, for example, trace, fractional anisotropy and mean, axial and radial diffusivity. The trace (Pierpaoli et al. 1996a) of the tensor is calculated as a sum of the eigenvalues

$$trace = \lambda_1 + \lambda_2 + \lambda_3.$$

The mean diffusivity (Pierpaoli et al. 1996a) is calculated as the average of the eigenvalues

$$MD = <\lambda> = \frac{\lambda_1 + \lambda_2 + \lambda_3}{3}.$$

Axial diffusivity (AD) is the diffusivity parallel to the fiber bundles. Axial diffusivity is the same as the eigenvalue related to the primary eigenvector

$$AD = \lambda_1,$$

and radial diffusivity (RD) is the diffusion perpendicular to the fiber bundles and is calculated as an average of the two eigenvalues

$$RD = \frac{\lambda_2 + \lambda_3}{2}$$

The fractional anisotropy (Basser et al. 1996) measures the magnitude of anisotropy and is given by

$$FA = \sqrt{\frac{3}{2}} \frac{\sqrt{(\lambda_1 - <\lambda>)^2 + (\lambda_2 - <\lambda>)^2 + (\lambda_3 - <\lambda>)^2}}{\sqrt{\lambda_1^2 + \lambda_2^2 + \lambda_3^2}}$$

FA values vary between 0 (isotropic diffusion) and 1 (infinite anisotropy).

An intuitive description of the diffusion tensor is that the diffusion boundary at each spatial location (voxel) is ellipsoidal. The diffusion boundary refers to the surface of the diffusion ellipsoid rather than the physical boundary that causes diffusion anisotropy of the boundary defined by the root mean square (RMS) displacements.

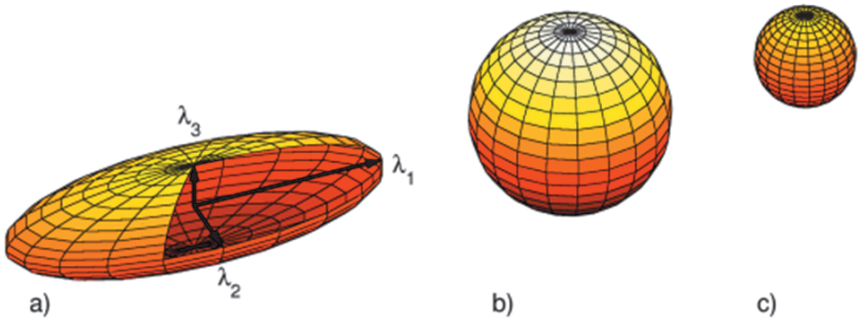

Figure 2. Diffusion ellipsoid. a) anisotropic diffusion, b) isotropic diffusion (unrestricted) c) isotropic diffusion (restricted). Diffusion tensor eigenvalues (λ1, λ2, λ3) are shown.

2.1.3 LIMITATIONS OF THE TENSOR MODEL

The tensor model appears to be a good approximation when the voxel contains only a single fiber orientation and a relatively small b-value is used in image acquisition (Jones et al. 2013). However, these conditions do not always apply in vivo. In general, the partial volume effect (PVE) and inability of the model to cope with non-Gaussian diffusion are major limitations of the tensor model (Jones et al. 2013).

Diffusion is non-Gaussian if there is more than one principal orientation present in a voxel. For example, the voxels can contain multiple fiber populations, bending fibers, and other deviations from the parallel fiber bundle assumption (Jones et al. 2013). Behrens et al. (2007) estimated that over third of white matter voxels have a multiple fibre crossing configurations when FA is larger than 0.1 (Behrens et al. 2007). This might be underestimation as Jeurissen et al. (2012) estimated that the proportion is as high as 90 percentage (Jeurissen et al. 2012). Therefore, we need higher order models to be able to overcome the shortcomings of the tensor model. For example, High Angular Resolution Diffusion Imaging (HARDI) has been developed to describe non-Gaussian distributions (Tuch et al. 2002).

The diffusion parameters may be biased so that measures of diffusivity (MD, AD and RD) will be increased and measures of anisotropy will be decreased, if the voxel contains cerebrospinal fluid (CSF) in addition to tissue (Metzler-Baddeley et al. 2012). CSF –based contamination artefacts are greater in areas with low FA compared to areas with high FA-values (Metzler-Baddeley et al. 2012). However, FA-values are more reliable and less partial volume error prone compared to measures of diffusivity (Metzler-Baddeley et al. 2012). Especially voxels in periventricular regions and around the perimeters of the brain parenchyma are susceptible to CSF –contamination based partial volume effects (Metzler-Baddeley et al. 2012). The impact of CSF –contamination is dependent on the b-value: the error in diffusion values is larger in low b-values (b~750 smm−2), and improves as the b-value is increased (b~1,500 smm−2) (Metzler-Baddeley et al. 2012).

The tensor model does not take in to account deviations from the single-exponential decay (Jones et al. 2013). However, based on observations the signal decay is non-monoexponential. This observation has led to the suggestions that the nervous tissue fall into at least two distinct populations, that have different diffusion coefficients (Jones et al. 2013). It is suggested that the slow component origins from the intra-axonal water where diffusion is restricted and the fast component originates from the extra-axonal space where diffusion is just hindered (Cohen and Assaf, 2002) (Jones et al. 2013). Different alternative models have been suggested to explain these different compartments such as Composite Hindered and Restricted Model of Diffusion (CHARMED). In CHARMED, the hindered diffusion in the extracellular space and within cell bodies is modeled by a diffusion tensor (Jones et al. 2013).

Typical resolution in DTI study is on the order of 1.5–2.5 isotropic mm (Jones et al. 2013). This is relatively low compared to clinical MRI imaging. Increasing spatial resolution is important, for example in order to minimize the number of voxels containing multiple fiber populations (Jones et al. 2013). However, SNR is one constraint for the spatial resolution of diffusion weighted images as too low SNR results completely unreliable data. It has been suggested that the SNR should never be below about 3:1 in any of the diffusion-weighted images (Jones and Basser, 2004). Descoteaux et al. (2009) suggest 10:1 as a safe minimum for the SNR (Jones et al. 2013). If the SNR is 10:1 for the b-value of 1000 smm−2, the non-diffusion-weighted SNR must be (10/0.37)= 27:1 (Jones et al. 2013).

It is clear that DTI has limitations due to the simplified model. Nevertheless, when the effects of complex fiber architecture, CSF –contamination and SNR on the diffusion values are corrected or taken in to account in the interpretation of the results, DTI remains a powerful tool to study white matter in vivo.

2.1.4 ANALYZING METHODS OF DIFFUSION TENSOR IMAGING

2.1.4.1 Region-of-interest (ROI)

Diffusion tensor images can be analyzed by measuring parameter values from a specified region-of-interest (ROI). The selection of the ROI can be made based on the anatomical structures of the individual patient. However, this means that the ROIs have to be drawn separately for each patient and each brain white matter structure. The ROI method is relatively simple and clinically feasible.

ROI analysis requires prior knowledge of the area of interest and can be time-consuming when analyzing large patient populations. Intra- and interobserver reproducibility can vary between different patient populations and between different brain structures. The accuracy of ROI locations is also based on the anatomical knowledge of the researcher performing the measurements. Good intra- and interobserver reproducibility of parameter value measurements has been reported using anatomically shaped ROI selection (Bonekamp et al. 2007). Reproducibility can be classified as excellent when intraclass correlation

coefficient (ICC) is greater than 0.75, fair to good when ICC is more than 0.4 but less than 0.75 and poor when ICC is less than 0.4 (Fleiss 1986). Even though this kind of classification is not evidence based, it provides a useful 'benchmark' for clinical research.

The subjectivity of ROI selection can be overcome by using ROI templates. However, this requires the images from individual patients to be registered to general anatomical atlases, such as the AAL atlas (Tzourio-Mazoyer et al. 2002) or the Talairach atlas (Lancaster et al. 1997, Lancaster et al. 2000). Another alternative is the use of tractography methods for ROI selection. The reproducibility of tractography based analysis has proven to be better than that of manual ROI analysis (Partridge et al. 2005).

2.1.4.2 Voxel-based analysis

Voxel-based analysis can be used to analyze structural brain differences from DTI parametric images. The statistical analysis can be performed voxelwise in the whole brain without prior knowledge of the areas of interest. Voxel-based analysis of DTI data can be carried out, for example, using tract-based spatial statistics (TBSS) (Smith et al. 2006), which is part of the FMRIB (Functional MRI of Brain) Software Library (FSL) (Smith et al. 2004) or using voxel-based morphometry (VBM) using Statistical Parametric Mapping (SPM) (Frackowiak et al. 1997).

In voxel-based analyses, patient images are spatially normalized to the same standard space. The spatial normalization is performed by registering each of the images to the same template. The VBM analysis is susceptible to misalignment errors, for example (Ashburner et al. 2001, Bookstein 2001). The images must also be smoothed. The optimal smoothing extent has not been found, and it is known that varying the size of the smoothing filter in VBM can lead to different analysis results (Jones et al. 2005).

The TBSS method tries to overcome these two issues observed in VBM analysis; TBSS does not require perfect alignment and no smoothing is required (Smith et al. 2006). The included template (for FSL) is FMRIB58_FA. The template is based on high resolution images from 20–50 year-old men and women (Webster 2012a). The template is not suitable for some study subjects such as young children or infants. In these cases, a study-specific template can be used (Ball et al. 2010). Even, if a study-specific template is chosen, the images are affine-aligned into an MNI152 standard space (Webster 2012b). The analysis is based on 'thinning' the mean FA image that has been created in the alignment procedure. This is practically an additional alignment step. This 'thinned' FA image is referred to as the FA skeleton and represents the center of all white matter fiber tracts common to all of the patients in a study. This skeletonization is performed perpendicular to local tract structures using non-maximum-suppression (Smith et al. 2006). All of the data is then projected onto the skeleton by taking the FA value from the center of the nearest relevant tract (Smith et al. 2006). The disadvantage is that the TBSS analysis is restricted to

white matter. Voxelwise statistical analysis can be performed using nonparametric statistics such as permutation testing to perform whole-brain DTI analysis (Chung et al. 2008).

In FSL the permutation testing is performed using Randomise tool. Performing all possible permutations is often not feasible. Instead, a random sample of possible permutations can be used (Monte Carlo permutation test) (Nichols 2013). On average the Monte Carlo permutation test will provide similar results to carrying out all possible permutation (Nichols 2013). The confidence limits for p=0.05 for 5,000 permutations are ±0.0062 and for 10,000 permutations 0.0044.

2.1.4.3 Tractography

Tractography involves following one or more white matter bundles. Using tracking algorithms, 3D models can be formed from white matter tracts (Basser et al. 2000b, Conturo et al. 1999). The most common techniques are streamline deterministic fiber tracking and probabilistic fiber tracking (Mori et al. 1999).

In deterministic tractography algorithms, it is assumed that the principal eigenvector is parallel to the main direction of the fibers in every voxel (Mori et al. 1999, Mori et al. 2002, Xue et al. 1999). The algorithm computes a trajectory starting for the user-defined starting ROI. When the fiber trajectory reaches the edge of the voxel, the direction of the trajectory is changed to match the primary eigenvector of the next voxel (Mori et al. 2002). The tracking is ended if the turning angle between adjacent voxels is too large, or if the FA-value is less than a predefined limit. Multiple ROIs can be used to differentiate different white matter tracts (Mori et al. 2002). The main limitation of the deterministic tracking approach is cases where the diffusion does not have a main direction, for example in voxels where white matter pathways branch or cross (Mori et al. 1999) or if the diffusion is planar ($\lambda 1 \approx \lambda 2 \gg \lambda 3$).

Probabilistic fiber tracking methods are used to overcome these shortcomings and the expected uncertainty in the tracking algorithm. The probability density function of the orientation of a neuronal fiber can be estimated using an empirical function based on the FA (Parker et al. 2003) or bootstrap statistics (Lazar et al. 2005).

In addition to the visualization of white matter fiber tracts, quantitative analysis can be performed. The mean diffusion parameter values for the whole tract can be determined from the selected white matter tracts. As the tracts may have heterogeneous structural characteristics (Berman et al. 2005), it is possible to segment the white matter tract in to several regions and perform quantitative analysis separately on different segments.

2.2 PRETERM INFANTS

2.2.1 CONCEPTS AND DEFINITIONS

2.2.1.1 Prematurity and birth weight

The World Health Organization (WHO) defines that infants born before gestational week 37 are considered preterm (Chiswick 1986), infants born before gestational week 32 are considered very preterm, and infants born before gestational week 28 are considered extremely preterm (Tucker et al. 2004).

Infants can also be classified based on their birth weight. Infants are defined as low birth weight infants, if the birth weight is 2,500 g or less. Very low birth weight (VLBW) is defined as birth weight less than 1,501 g and extremely low birth weight (ELWB) if birth weight is less than 1,000 g. Low birth weight may be due to prematurity, being born small for gestational age (SGA), or both. (Tucker et al. 2004)

2.2.1.2 Small for Gestational Age (SGA)

The birth weight z-score is defined as an infant's birth weight compared to the expected average weight of infants of the same gender born at the same gestational age. The difference is expressed as a standard deviation from the mean of gender- and age-specific Finnish national growth charts.

An infant is defined as small for gestational age (SGA) if the birth weight z-score is less than -2 standard deviations (SD) from the mean. SGA infants are either constitutionally small or have had impaired intrauterine growth (Intrauterine-Growth-Restriction-infants, IUGR infants). IUGR infants are reported to have a more immature cortical microstructure and reduced volumes in the cerebral cortical grey matter (GM) and occipital volumes (Huppi et al. 2004, Inder et al. 2005, Thompson et al. 2007).

2.2.1.3 Catch-up growth

Catch-up growth is seen as rapid increase in weight, length and head circumference (HC). It is defined as reaching the z-score above -2 SDs of the reference population (Lee et al. 2003). Catch-up growth is usually achieved at 2–3 years of age. In some cases, catch-up growth may continue into adolescence (Euser et al. 2008).

2.2.2 NORMAL BRAIN MATURATION

Brain development begins in the third gestational week (Tau et al. 2010). By the end of the eighth gestational week, the primitive brain and central nervous

system have been formed (Stiles et al. 2010). The brain maturation period starts from the ninth gestational week and is characterized by the processes of neuron production, migration, and differentiation. Most neurons are produced in the ventricular zone and migrate radially to the developing neocortex. The majority of neurons have been produced by mid-gestation (Stiles et al. 2010).

Neuronal migration to the cerebral cortex is complete by 20–24 gestational weeks. However, glial cell migration continues even after this. This results in an increase of the surface area of the cortex as cortical folding develops (Ajayi-Obe et al. 2000). Once positioned in the cortex, neurons develop neuronal processes (axons and dendrites) that form the fiber pathways of the brain neural networks. The major fiber pathways make up the brain white matter.

Histologically, myelination starts at about 25 gestational weeks (Brody et al. 1987). However, myelin is microscopically seen in the ascending thalamocortical tracts and the descending corticospinal tracts by 32 gestational weeks, in the striatum, and pre- and postcentral gyri by 35 gestational weeks, and in the anterior limb of the internal capsule and optic radiation by 37 gestational weeks. At term age, using conventional T1 and T2 weighted MR images, myelin can be seen in the thalamus, anterior and posterior limb of the internal capsule, part of the globus pallidus, the optic and acoustic radiations as well as in the pre- and postcentral subcortical white matter (WM) (Sie et al. 1997). Myelination continues after birth: myelination is rapid in the first two postnatal years and continues more slowly into adulthood.

2.2.3 CONVENTIONAL MRI AND TYPICAL PATHOLOGICAL MR FINDINGS IN PREMATURITY AT TERM AGE

Magnetic resonance imaging has been used to study the maturational processes that take place after birth. In addition to illustrating normal developmental changes, MRI can be used to study brain lesions that can cause poor neurodevelopmental outcomes. Conventional MR imaging of preterm infants typically contains T1, T2, and diffusion-weighted and hemo or susceptibility weighted sequences.

It is known that the T1 and T2 relaxation times are much longer for infants than adults (Jones et al. 2004, Nowell et al. 1987). Brain maturation alters the signal intensity of the white matter in T1- and T2-weighted images. The signal intensity changes in T1- and T2-weighted images have been associated with decreasing brain water content and the forming of the myelin membrane around axons and neurons (Barkovich et al. 1988). Atlases exist that can be used to check and compare the brain appearance to reference images of normal infants at the same age (Barkovich 2000).

The severe pathological finding in a preterm infant is periventricular leukomalacia (Volpe 2009). Some of the fiber bundles can be completely destroyed and in any case this hypoxic-ischemic white matter injury can impact on white matter maturation (Volpe 2009). Damaged areas are typically near posterior limb of the internal capsule and also the corpus callosum can be

damaged. Another important pathological finding in a preterm infant is germinal matrix bleeding, which is classified into grades I-IV (Leung 2004). This bleeding can lead to serious situations such as hydrocephalus (Ballabh 2010). Other reported findings in MRI are parietally and occipitally located white matter lesions, as well as cortical, subcortical, and basal ganglia abnormalities, followed by atrophy of these parts of the brain (Leijser et al. 2009).

2.2.4 OUTCOME OF PREMATURE OR SGA BIRTH

Preterm infants are at greater risk for mortality than term born infants. The absolute mortality by one year of age was 12.4 % for live-born very low gestational age (VLGA) or VLBW infants (born below 32 weeks or below 1,501 g in Finland 2005–2007, lethal anomalies excluded) (Lehtonen et al. 2011).

In addition to increased mortality, preterm infants are at greater risk than term infants of developmental problems such as acute respiratory, gastrointestinal, immunological, central nervous system, hearing, and vision problems, as well as long-term motor, cognitive, visual, hearing, behavioral, social-emotional, health, and growth problems (Behrman 2007). In live-born VLGA/VLBW infants born below GA < 32 weeks or a birth weight of < 1,501 g, born in Finland between 2000 and 2003, the rate of cerebral palsy (CP) was 6.1%, seizures 3.0%, hearing loss 2.5%, visual disorders 3.8%, and other ophthalmological problems 13.4% (Korvenranta et al. 2009).

SGA infants are reported to have increased risk of minor neurological dysfunctions and reduced scores in developmental tests in childhood (Lundgren et al. 2008, Lundgren et al. 2004). In addition, low birth length and head circumference also increased the risk of subnormal intellectual and psychological performance in adulthood (Lundgren et al. 2004).

Greater weight gain before term age is reported to be associated with better outcomes (Belfort et al. 2011). In previous studies, catch-up growth in weight, length, and particularly head circumference, has been shown to be important for neurodevelopmental outcomes (Belfort et al. 2011, Ehrenkranz et al. 2006, Franz et al. 2009, Lundgren et al. 2001). In particular, lacking height catch-up is associated with poorer outcomes in lower intellectual and psychological performance in adult men (Lundgren et al. 2004). Frisk et al. showed that SGA infants with delayed intrauterine brain growth showed deficient cognitive abilities and literacy skills compared to full term infants despite their catch-up growth between birth and nine months of corrected age (Frisk et al. 2002). Still, they reported that SGA infants that had good catch-up growth performed better compared to SGA infants without catch-up growth (Frisk et al. 2002). Similar results were reported by Lundgren et al., where SGA male infants who had good catch-up growth performed better on intellectual performance tests compared to SGA infants without catch-up growth (Lundgren et al. 2001, Lundgren et al. 2004).

2.3 DTI OF WHITE MATTER MATURATION

2.3.1 NORMAL WHITE MATTER MATURATION

Quantitative measures from DTI reflect brain maturation processes, such as myelination, axonal integrity, and the general organization and alignment of groups of axons in white matter tissue (Beaulieu 2002, Dubois et al. 2008a, Dubois et al. 2008b, Mori et al. 2006, Mukherjee et al. 2002, Neil et al. 2002). In healthy infant, normal white matter maturation is characterized by increasing fractional anisotropy and decreasing mean diffusivity with increasing age (Dubois et al. 2006). Hermoye et al. and Saksena et al. reported rapid increases of FA in cerebral white matter during the first year after birth (Hermoye et al. 2006, Saksena et al. 2008). After this, postnatal growth is characterized by slower increases up to 11 years (Saksena et al. 2008). For MD, a sharp decrease is observed up to the age of 2 years (Saksena et al. 2008).

The white matter maturation stage varies between brain structures. At term age, deep white matter (posterior limb of internal capsule, genu, and splenium of corpus callosum) is more mature compared to peripheral white matter (associational white matter underlying prefrontal, and posterior parietal cortex) (Provenzale et al. 2007). Boujraf et al. showed an association between increasing anisotropy and myelination during the first year of life (Boujraf et al. 2002). The myelination of the posterior limb occurs during the first months after birth. Myelination of the anterior limb of the internal capsula, optical radiation, and splenium occurs up to 4 months (Boujraf et al. 2002). Provenzale et al. showed that myelination occurs earlier in the splenium than in the genu (Provenzale et al. 2012). The myelination of the frontal white matter starts at the sixth month and continues thereafter (Boujraf et al. 2002).

2.3.2 PRETERM BIRTH: LONGITUDINAL GROWTH

Maturational changes assessed with diffusion parameters show similar trends with age in preterm infants to those observed in term born infants. In the majority of white matter structures FA increases and MD, $\lambda 2$, and, $\lambda 3$ decrease with increasing age (Aeby et al. 2009, Berman et al. 2005, Berman et al. 2009, Dudink et al. 2007, Miller et al. 2002, Neil et al. 1998).

Berman et al. showed associations between FA and increasing age in the motor and sensory pathways between 28 and 43 weeks of gestation (Berman et al. 2005). Increasing FA with increasing age was shown in the optic radiation between 29 to 41 weeks of gestation (Berman et al. 2009). Dudink et al. demonstrated an association between FA and age in the posterior limb of the internal capsule in preterm infants born between 25 and 32 weeks of gestational age (Dudink et al. 2007). They did not find correlations between FA and age in other studied structures (anterior limb of internal capsule, external capsule, optic radiation, genu and splenium of the corpus callosum). Aeby et al. found that, between GA 34 and 41 weeks, FA increases with age in the subcortical projections from the frontal (motor and premotor areas) and parietal cortices,

the centrum semiovale, the anterior and posterior part of the internal capsula, the optic radiations, the corpus callosum, and the thalami (Aeby et al. 2009). Miller et al. demonstrated that anisotropy increased with age in the basal ganglia, thalamus, calcarine gray matter, hippocampus, corticospinal tract, frontal and posterior white matter, and optic radiations in preterm infants between 27.5 and 38 weeks post conception (Miller et al. 2002).

The results, reported for MD, are confounding. Miller et al. showed that MD decreases with increasing age in the same areas (basal ganglia, thalamus, calcarine gray matter, hippocampus, corticospinal tract, frontal and posterior white matter, optic radiations) in which anisotropy increased with age between GA 27.5–38 weeks, and Neal et al. showed a negative correlation with age and MD (GA: 31-41 weeks) (Miller et al. 2002, Neil et al. 1998). Berman et al. reported that MD decreases after premature birth (GA: 29-41 weeks) (Berman et al. 2009). However, Dudink et al. and Aeby et al. reported that MD did not have a significant correlation with age in any of the studied structures (Aeby et al. 2009, Dudink et al. 2007) .

Berman et al. reported that transverse diffusion (λ2 and λ3) in the motor and sensorimotor tract decreased with increasing age at a higher rate than axial diffusion (λ1) (Berman et al. 2005). In a later study, it was reported that AD and RD in optic radiation decrease after premature birth (GA: 29 to 41 weeks) (Berman et al. 2009). However, Partridge el al reported contradictory results, when they showed that the major eigenvalue (λ1, AD) showed a negative correlation with age in several white matter structures (the centrum semiovale, external/extreme capsule, and internal capsule) (Partridge et al. 2004).

Bonifacio et al. were not able to show an independent effect between extremely premature birth and white matter maturation using serial DTI measurements (Bonifacio et al. 2010). They concluded that infants born extremely premature have a similar possibility of normal brain development as infants born at a later gestational age. They concluded that premature birth alone is not a strong determinant of brain development (Bonifacio et al. 2010).

2.3.3 PRETERM BIRTH: DTI AT TERM AGE

The results regarding the effect of prematurity on white matter maturation at term age have been contradictory. Some of the studies have reported that white matter maturation is independent of prematurity (Bonifacio et al. 2010, de Bruine et al. 2011); others have reported that preterm infants have delayed brain maturation compared to term infants (Anjari et al. 2007, Hasegawa et al. 2011, Huppi et al. 1998, Rose et al. 2008, Thompson et al. 2011), and a few have reported that preterm infants show accelerated white matter maturation compared to term infants (Gimenez et al. 2008, Rose et al. 2008).

According to Bonifacio et al., extreme premature birth (GA < 26 weeks) is not associated with impaired development of brain microstructures (frontal and parietal WM, corticospinal, optic radiation, PLIC, thalamus, basal ganglia, hippocampus, calcarine gray) when co-morbid conditions (moderate to severe

brain injury) are accounted for (Bonifacio et al. 2010). They performed their analysis using the ROI method. Similar results were reported by de Bruine et al., using tractography, who found no associations between DTI parameters and GA at birth (GA ≤ 32 weeks) in white matter tracts passing through the PLIC and corpus callosum (de Bruine et al. 2011).

According to Huppi et al., using the ROI method, preterm infants showed delayed white matter maturation in their cerebral white matter (the posterior limb of the internal capsule and the central white matter) compared to term infants at term age (Huppi et al. 1998). Anjari et al. used TBSS and reported lower FA values to be found in regions within the centrum semiovale, frontal white matter and the genu of the corpus callosum (Anjari et al. 2007). They also found reduced FA values in infants born less than or equal to 28 weeks GA compared to term infants in additional brain areas: the posterior limb of the internal capsule, the external capsule and in the different parts of the corpus callosum (the isthmus and middle portion of the body) (Anjari et al. 2007). Both Hasegava et al. and Thomson et al. reported findings on the maturation of corpus callosum using tractography (Hasegawa et al. 2011, Thompson et al. 2011). Thompson et al. showed that very premature infants have lower FA and higher MD and RD values than term infants when accessing the entire corpus callosum (Thompson et al. 2011). Preterm infants had also higher AD values in the genu compared to term infants. However, in the splenium, all significant differences were lost after adjusting the analysis with GA using MRI (Thompson et al. 2011). Interestingly, Hasegawa et al. showed that the degree of premature birth affects the maturation of the splenium (Hasegawa et al. 2011). They showed that preterm infants (born 23-25 GA) exhibited lower FA in the splenium than preterm infants born at a later gestational age (26-29 GA and 30-33 GA) (Hasegawa et al. 2011). Rose et al., using TBSS, reported increased FA values in term infants compared to very preterm infants (GA < 29 weeks) in regions within the corpus callosum, corona radiata, and centrum semiovale (Rose et al. 2008).

Surprisingly, Rose et al. reported increased FA values in specific white matter tracts in preterm and very preterm infants compared to term infants. However, they suspected that this delayed white matter maturation of the term infants was artifactual, because behavioral studies did not support these findings (Rose et al. 2008). Gimenez et al., using VBM, have also reported that preterm infants have higher FA values in the sagittal stratum compared to controls at term age (Gimenez et al. 2008). This finding suggests that white matter maturation may be accelerated in preterm infants.

2.3.4 DTI OF DISTURBED ANTENATAL GROWTH

The impact of disturbed antenatal growth on white matter maturation and later outcomes has not been widely reported. In animal studies, it has been shown that intra uterine growth restriction (IUGR) decreased FA values in rabbits compared to those with normal antenatal growth (Eixarch et al. 2012). Previous clinical studies have demonstrated that IUGR infants have microstructural

alterations in the parieto-occipital and frontal cortex as assessed with both MD and FA values (Huppi et al. 2004), and higher MD values in the internal capsule compared to controls (Sizonenko et al. 2006). These findings indicate that at term age, IUGR infants have more immature white matter compared to infants with normal antenatal growth (Huppi et al. 2004, Sizonenko et al. 2006).

Brain maturation is a complex process and any disturbance in this process could affect the white matter pathway (Kostovic et al. 2010, Ramenghi et al. 2011). In previous studies, any white matter abnormalities (Liu et al. 2012, Skiold et al. 2010), or diffuse excessive high signal intensity (DEHSI) (Counsell et al. 2006, Skiold et al. 2010) have been associated with changes in diffusion parameter values. In general, MD values are reported to decrease quickly after injury in the case of cell injury and cytotoxic edema (Neil et al. 2002). Even though MD values decrease following the injury, eventually the MD increases to a greater than normal value. However, in the case of vasogenic edema, increased diffusion was observed even in the early phase (Ebisu et al. 1993). Anisotropy values are reported to reduce from the normal level (Drobyshevsky et al. 2007, Miller et al. 2002, Neil et al. 2002).

2.4 PREDICTING CLINICAL OUTCOMES USING DTI

Previous studies have reported positive associations between FA-values (indicating good white matter maturation) at term age and good cognitive, fine-motor, and gross-motor performance at 2-year corrected age (Van Kooij et al. 2012) as well as good visual fixation performance and higher fractional anisotropy (Berman et al. 2009). The organization and maturation of the arcuate fasciculus and the cortico-spinal tract have also been used to explain later functional lateralization (Dubois et al. 2009, Liu et al. 2010). At term age, lower FA values in the right PLIC and splenium have been associated with abnormal neurodevelopment (Arzoumanian et al. 2003, Rose et al. 2009).

The confounding clinical factors, such as gestational age at birth, birth weight, catch-up growth or lack thereof, and brain injuries, will still provide future challenges. Technical limitations of DTI, such as partial volume effect, might be especially important to correct in this particular patient group as white matter structures are small and FA values are low (Metzler-Baddeley et al. 2012, Vos et al. 2011). Using correction either in image acquisition, such as fluid attenuated inversion recovery (FLAIR) or cardiac gating, or in the post processing phase, such as Free Water Elimination (FWE), might be necessary when assessing the future outcomes of preterm infants (Metzler-Baddeley et al. 2012).

3 OBJECTIVES OF THE STUDY

The aim of this study was to investigate the feasibility and usability of ROI and tract-based spatial statistics (TBSS) analysis of the diffusion tensor images of the white matter of the brains of preterm infants at term age. The specific objectives of this study were:

1. To investigate the intraobserver and interobserver reproducibility of fractional anisotropy and mean diffusivity measurements performed with ROI analysis in several white matter areas of preterm infants at term age.

2. To compare the maturity of white matter at term age in preterm infants born at different gestational ages. To study the correlation between brain white matter maturation and birth weight relative to gestational weeks using ROI analysis.

3. To compare whole-brain white matter maturation using the TBSS method between preterm infants who were born small for gestational age and preterm infants whose weight was appropriate for gestational age.

4. To assess the effect of postnatal growth from birth to term age on brain white matter maturation using the TBSS method.

4 METHODS

4.1 SUBJECTS

4.1.1 THE INCLUSION CRITERIA

The inclusion criteria for this study were (1) gestational age below 32 weeks or VLBW (birth weight less than 1,501 g) and (2) imaged with a 1.5 T magnetic resonance imaging (MRI) system at term age (40 gestational weeks, GW). The brain imaging for this study was performed between June 2004 and December 2006. A total of 132 infants met the inclusion criteria.

These studies are part of the Development and Functioning in VLBW infants from Infancy to School Age (PIPARI) study conducted at Turku University Hospital. The study protocols were approved by the Ethics Review Committee of the Hospital District of South-West Finland. All families provided informed consent.

4.1.2 THE EXCLUSION CRITERIA

The exclusion criteria for all studies (I, II, III and IV) were: (1) the infant had died during the neonatal period [n=17]; (2) major congenital anomalies or recognized syndromes [n=2]; (3) DTI that was incorrectly acquired or not acquired at all [n= 21]; (4) infant lived outside the hospital district [n=2]; (5) parents did not speak Finnish or Swedish [n=5]; and (6) families refused to participate [n=9] (Maunu et al. 2006). A total of 76 preterm infants were accepted for Study I and Study II.

In Studies III and IV additional exclusion criteria were added: (7) movement artifacts in acquired images [n=20]; (8) major brain pathology (intraventricular hemorrhage, IVH, grades 3 to 4, hemorrhage of the brain parenchyma, white matter cysts, abnormal signal intensities in the T1 or T2 weighted images in the cortex, basal ganglia, thalamus, cerebellum or internal capsule, abnormality of the corpus callosum, an extracerebral space width of 6 mm or more, and ventriculitis) in conventional magnetic resonance, images [n=16]. Brain pathologies were classified based on conventional MR images by a senior neuroradiologist Riitta Parkkola, the second supervisor of this thesis. A total of 40 preterm infants were accepted for Studies III and IV. In the data analysis, the image registration process failed in three infants and one infant had missing clinical data. The final study population consisted of 36 preterm infants.

4.2 STUDY DESIGN

Table 1 shows the clinical data for the 76 infants studied (Study I and Study II) and the 36 infants studied (Study III and Study IV). The myelination status (Study IV), confirmed by conventional imaging at term age, was not delayed.

Table 1. Clinical data for the study subjects

	infants (n=76) Study I and II	infants (n=36) Study III and IV
GA at MRI (weeks), mean ± SD	40.0 ± 0.6	39.9 ± 0.4
Birth weight (g), mean ± SD	1,289 ± 362	1,435 ± 296
Birth weight z-score, mean ± SD	-1.45 ± 1.59	-0.99 ± 1.38
Head circumference z-score, mean ± SD	-0.72 ± 1.56	-0.35 ± 1.57
Maternal age (years), mean ± SD	32 ± 5	31 ± 5
GA at birth (weeks), mean ± SD	30.0 ± 2.4	30.4 ± 1.9
Apgar score, median [lower quartile, upper quartile]	8 [7,9]	8 [7,9]
Antenatal steroids (no/yes)	9 / 67	2 / 34
Postnatal steroids (no/yes)	4 / 72	36
Umbilical artery pH ≥ 7	70 *	35 **
Cesarean section (no/yes)	46 / 30	13 / 23
Pre-eclampsia (no/mild/severe)	52 / 3 / 21	29 /1/6
Absent or reversed flow in the umbilical artery (no/yes)	22/ 6 ***	7 /1 ****

Data missing from 6 (*), 1 (**), 48 (***), and 28 (****) infants.

4.3 MAGNETIC RESONANCE IMAGING

The MR imaging was performed with a 1.5 T MRI system (Gyroscan Intera CV Nova Dual, Philips medical systems, the Netherlands) using a SENSE head coil.

MRI was performed at term age. Imaging was performed during postprandial sleep without any pharmacological sedation. The infants were swaddled to calm them and to reduce movement artifacts in the images. A pulse oximeter was routinely used during MRI. A physician attended the examination to monitor the infant, if necessary. Ear protection was used (3M Disposable Ear Plugs 1100,

3M, Brazil and Wurth Hearing protector art.-Nr. 899 3000 232, Wurth, Austria).

The clinical MRI protocol included conventional T1, T2 and FLAIR sequences. The imaging parameters were for the T2 –weighted turbo spin echo (TSE) sequence: TR varied with the number of slices and TE was 120 ms. The reconstructed voxel size was 0.78 mm x 0.78 mm x 4 mm. The imaging parameters were for T1 –weighted TSE sequence: TR varied (from 494 ms to 565 ms) with the number of slices, TE was 14 ms. The reconstructed voxel size was 0.78 mm x 0.78 mm x 4 mm. The imaging parameters were for a FLAIR sequence: TR was 3,500 ms, TE 15 ms and inversion time (TI) was 400 ms. The reconstructed voxel size was 0.70 mm x 0.70 mm x 4 mm.

Diffusion-weighted imaging was conducted using single-shot echo planar imaging (EPI) with SENSE. SENSE reduction was 2. The imaging matrix was 112 x 89 and the reconstructed voxel size was 0.78 mm x 0.78 mm x 5 mm. The gap between slices was 1 mm. Total number of slices varied between 15 and 22. The number of signal averages was 2 and the EPI factor was 47. The TR was the shortest possible (varied from 2,264 ms to 4,420 ms) and the TE was 68 ms. The b-values were 0, 600 and 1,200 s/mm^2. In total, 15 diffusion encoding gradient directions were used. Fat suppression was done using spectral presaturation with inversion recovery (SPIR). The phase encoding was done in anterior-posterior direction and the receiver bandwidth was 19.6 Hz/pixel. The total imaging time ranged between 2 minutes 24 seconds and 4 minutes 43 seconds.

4.4 GROWTH ANALYSIS

4.4.1 ANTENATAL GROWTH ANALYSIS

The infants were measured at birth as part of their routine care and follow-up. The birth weight of the infants was compared to the expected average weight of infants of the same gender born at the same gestational age. The difference is expressed as standard deviations from the mean of gender- and age-specific Finnish national growth charts (birth weight z-score).

If the birth weight z-score is less than -2 SDs from the mean, the infant is classified as a small for gestational age (SGA) infant. Otherwise, the infant is classified as an appropriate for gestational age (AGA) infant. In total, nine infants were born SGA (Study III). In the TBSS analysis GA was used as a confounding covariate.

4.4.2 POSTNATAL GROWTH ANALYSIS

The infants were measured at birth and at term age as part of their routine care and follow-up. The z-scores for weight, length and HC were calculated using

gender and age-specific Finnish national growth charts at birth and at term age (Pihkala et al. 1989, Sorva et al. 1990). The z-scores are shown in Study IV.

The z-score change rate between birth and term age was calculated and divided by postnatal age in weeks to minimize variation caused by differences in gestational age. The z-score of birth weight was used as a confounding covariate.

4.5 DATA ANALYSIS

4.5.1 REGION OF INTEREST ANALYSIS

PRIDE V4 Fiber Tracking 4.1 beta 4 (Philips Medical Systems, Best, The Netherlands) software was used for the image analysis. ROIs were drawn based on anatomical structures on the directionally encoded anisotropy color maps. Only images with b-values of 0 and 600 s/mm² were used in the ROI analysis. Images with b-value 1,200 s/mm² were not used in the analysis due to technical limitations of the PRIDE software. An image with a b-value of 0 s/mm² was used as an anatomical reference image.

The ROIs were drawn on the genu and splenium of the corpus callosum, the posterior part of the internal capsule, the corona radiata, optic radiation, and the inferior colliculus. Symmetrical structures were measured bilaterally. The fractional anisotropy and mean diffusion were measured. ROI locations are shown in Figure 3.

ROIs were drawn twice by one observer (Observer A, medical physicist supervised by neuroradiologist with 2 years' experience in neuroradiology) to evaluate intraobserver reproducibility and once by a second observer (Observer B, senior neuroradiologist with 13 years' experience in neuroradiology) to evaluate interobserver reproducibility.

None of the patients or images was removed before ROI analysis. Observers chose independently acceptable image quality. Only images that both observers classified as having sufficient image quality were accepted for this study (Study I and Study II). Because of this, the number of ROI measurements varied between structures: genu (n=65), splenium (n=62), right (n=63) and left (n=64) internal capsule, corona radiata (n=60), optic radiation (n=66), and inferior colliculus (n=63).

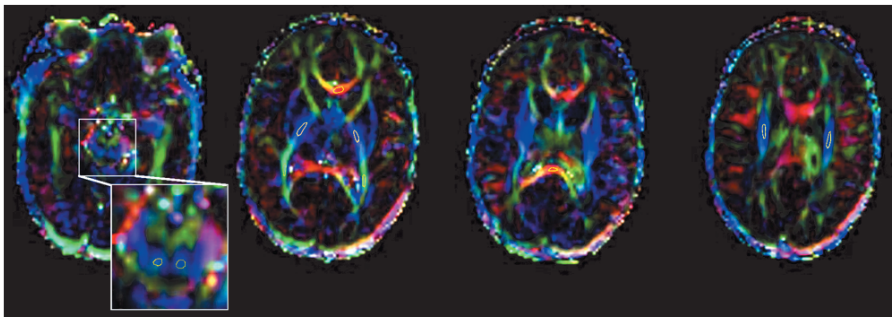

Figure 3. Position of ROIs demonstrated on color-coded fractional anisotropy maps. ROI measurements were performed on the colliculus inferior, genu and splenium of the corpus callosum, internal capsule, optic radiation, and corona radiata.

4.5.2 STATISTICAL ANALYSIS OF THE ROI METHOD

The reproducibility of the ROI method was assessed using both the intra-class correlation coefficient and Bland-Altman proposed limits of agreement (Bland et al. 1986) (Study I).

Interobserver ICCs were calculated between Observers A and B and intraobserver ICCs were calculated between the first and second measurement of Observer A using repeated measurements ANOVA. Variation in ROI size was taken into account in the analyses and the association of ROI size and measurements was also assessed. Residuals were checked for justification of the analysis, and logarithmic or power transformations of the variables were used in the analyses when appropriate. $P < 0.05$ was considered statistically significant.

Reproducibility was classified as 'excellent' when ICC was greater than 0.75, 'fair to good' when ICC was greater than or equal to 0.4 but less than or equal to 0.75 and 'poor' when ICC was less than 0.4. Statistical analyses were performed using SAS System for Windows, version 9.1.3. (SAS Institute, Cary, NC, USA) software.

Bland-Altman scatter plots were created using GraphPad Prism 5.00 (GraphPad Software, San Diego California USA) software by plotting the difference between two measurements against the averages of the two measurements. The Bland-Altman scatter plots were visually inspected.

For antenatal growth analysis using the ROI method (Study II), statistical analyses were performed using general linear models that used gestational age at birth, birth weight z-score and brain pathology as independent variables. The gestational age at birth and birth weight z-score were used as continuous variables. The dependent variables were FA and MD.

Residuals were checked to justify the analyses. $P<0.05$ was considered statistically significant. Statistical analyses were performed using SAS for

Windows, Version 9.2 (SAS Institute, Cary, NC, USA) software. In the statistical analysis, when the FA and MD values were normalized relative to gestational age and birth weight, the brain pathology classified in three categories had no association with the measured diffusion tensor parameters.

4.5.3 TRACT-BASED SPATIAL STATISTICS

Voxelwise statistical analysis of the infant data was conducted using Tract-Based Spatial Statistics (TBSS) (Smith et al. 2006), part of the FSL (4.1.7) (Smith et al. 2004). The brain was extracted using BET (Smith 2002). FA and MD images were calculated by fitting a tensor model to the raw diffusion data using FMRIB's Diffusion Toolbox (FDT). AD and RD images were calculated using the fslmaths tool.

All subjects' FA data were then aligned to a study-specific target using a nonlinear registration tool (FNIRT) (Andersson et al. 2007a, Andersson et al. 2007b). A study-specific target was used because an infant target is not included in the FSL. Image registrations to target were confirmed using visual inspection. A threshold value of 0.2 was used in the analysis.

The mean FA image was created and thinned to create a mean FA skeleton, which represents the centers of all tracts common to the group. Each subject's aligned FA data was then projected onto this skeleton.

Statistical analysis was performed using a randomize tool with 5,000 permutations. Threshold-free cluster enhancement (TFCE) was used in the analysis to enhance cluster-like structures without needing to define an initial cluster-forming threshold or carry out a large amount of data smoothing (Smith et al. 2009). Results were corrected for multiple comparisons. Associations with $p < 0.05$ were considered as statistically significant. Areas were identified using the JHU White-Matter Tractography Atlas.

5 RESULTS

5.1 ROI METHOD (STUDIES I AND II)

5.1.1 FA AND MD VALUES

The measured FA and MD values varied between white matter structures and between observers. The measured FA and MD values in the genu and splenium, capsula interna, corona radiata, optic radiation, and colliculus inferior are shown in Figure 4. In the figures, the measured FA and MD values (median; 25th and 75th centiles) are shown with white (Observer A, first measurement), light gray (Observer A, second measurement) and dark gray bars (Observer B).

5.1.2 REPRODUCIBILITY OF ROI MEASUREMENTS

The reproducibility of the ROI method in infants was assessed using the intraclass correlation coefficient and Bland-Altman Plots. Reproducibility was determined in the genu and splenium of the corpus callosum, posterior limb of the internal capsule, corona radiata, optic radiation, and inferior colliculus.

5.1.2.1 ICC method

The intraobserver reproducibility of FA measured with ICC was fair to good. The reproducibility of MD was excellent in the genu of the corpus callosum and in the posterior limb of the internal capsule, and corona radiata. In the left optic radiation, reproducibility was excellent. In other structures, the intraobserver reproducibility of MD was fair to good.

The interobserver reproducibility of FA measured with ICC was found to be excellent in the splenium of the corpus callosum. Reproducibility was fair to good in the other structures. The reproducibility of MD was excellent in the splenium of the corpus callosum, the posterior limb of the internal capsule and the right corona radiata. In most of the structures, the reproducibility of MD was fair to good. The reproducibility was poor in the right inferior colliculus.

ROI size varied between observers significantly and quite systematically. Observer A's ROIs were always smaller than those of Observer B. Observer A's ROIs were smaller on the second measurement as compared with the first, on most of the structures. When intraobserver reproducibility was assessed using ICC, ROI size had a significant effect on FA values in the left inferior colliculus. For MD values, the effect was significant in the inferior colliculus and in the left posterior limb of the internal capsule. When interobserver reproducibility was assessed using ICC, ROI size had a significant effect on FA in the genu and splenium of the corpus callosum, the left posterior limb of the internal capsule, the right optic radiation and the inferior colliculus. ROI size had a significant

effect on MD values for the genu and splenium of the corpus callosum, the right posterior limb of the internal capsule, and the inferior colliculus.

The results of the ICC measurements are summarized in Table 2.

Table 2. Reproducibility for FA and MD

	Intraobserver ICC		Interobserver ICC	
	FA	MD	FA	MD
Genu of the corpus callosum	0.52	0.82	0.67[a]	0.60[a]
Splenium of the corpus callosum	0.62	0.74	0.81[a]	0.76[a]
Right internal capsule (posterior limb)	0.74	0.92	0.67	0.86[a]
Left internal capsule (posterior limb)	0.52	0.88[a]	0.58[a]	0.89
Right corona radiata	0.53	0.89	0.54	0.79
Left corona radiata	0.61	0.88	0.52	0.73
Right optic radiation	0.49	0.62	0.45[a]	0.70
Left optic radiation	0.75	0.79	0.47	0.70
Right inferior colliculus	0.68	0.67[a]	0.71[a]	0.24[a]
Left inferior colliculus	0.53[a]	0.65[a]	0.73[a]	0.72[a]

[a] The ROI size had a significant effect on FA and MD values.

5.1.2.2 Bland-Altman method

A Bland-Altman analysis showed good results for the studied white matter structures based on a visual review of the Bland-Altman scatter plots. The scatter plots showed no considerable bias and variance was independent of the mean value. The interobserver Bland-Altman scatter plots for the genu and splenium of the corpus callosum are shown in Figure 5, the posterior limb of the internal capsule in Figure 6, the corona radiata in Figure 7, the optic radiation in Figure 8, and the colliculus inferior in Figure 9.

The limits of agreement varied between structures. For interobserver Bland-Altman scatter plots, the limits of agreement are shown in the figures. For

intraobserver Bland-Altman scatter plots, the limits of agreement and bias values are shown in Table 3.

Table 3. Intraobserver results from Bland-Altman analysis.

	BIAS (FA)	LA (FA)	BIAS (MD)	LA (MD)
Genu of the corpus callosum	0.053	-0.162 to 0.267	-0.016	-0.195 to 0.163
Splenium of the corpus callosum	0.043	-0.169 to 0.254	-0.059	-0.422 to 0.305
Right internal capsule	-0.012	-0.115 to 0.091	0.001	-0.055 to 0.056
Left internal capsule	0.007	-0.136 to 0.149	0.004	-0.074 to 0.083
Right corona radiata	0.040	-0.095 to 0.174	-0.020	-0.130 to 0.089
Left corona radiata	0.040	-0.085 to 0.166	-0.023	-0.154 to 0.109
Right optic radiation	0.002	-0.116 to 0.121	-0.060	-0.445 to 0.326
Left optic radiation	-0.007	-0.094 to 0.080	-0.020	-0.259 to 0.219
Right inferior colliculus	-0.008	-0.114 to 0.098	0.026	-0.104 to 0.156
Left inferior colliculus	-0.001	-0.131 to 0.130	0.015	-0.140 to 0.171

5.1.3 GESTATIONAL AGE

The ROI method showed that gestational age at birth had no significant association with white matter maturation in any of the studied white matter areas at term age (Study II). Maturation of the white matter was assessed using FA and MD.

5.1.4 ASSOCIATION BETWEEN WHITE MATTER MATURATION AND DIFFUSION VALUES USING ROI METHOD

The birth weight z-score had a significant association with FA and MD at term age. FA values were associated positively with antenatal growth in the genu (P=0.012) and splenium (P=0.032) of the corpus callosum. MD values were associated negatively with antenatal growth in the splenium of corpus callosum (P=0.002) (Study II).

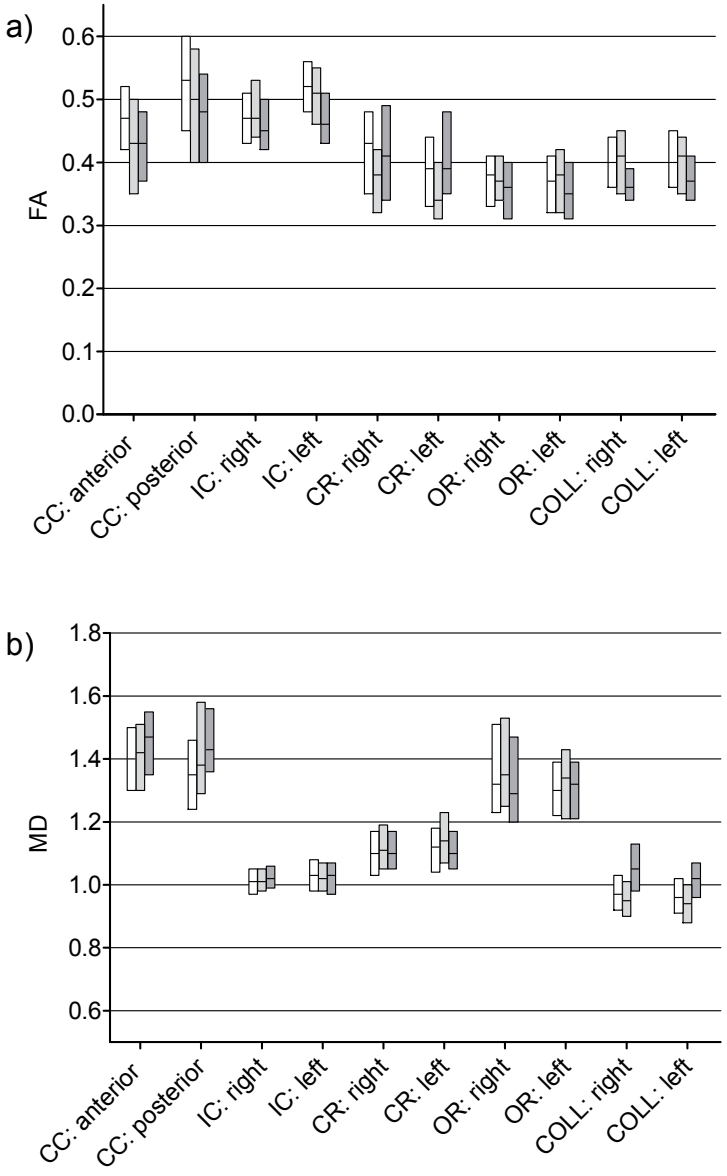

Figure 4. Measured fractional anisotropy (FA) and mean diffusivity (MD) values. Measured a) FA and b) MD values (median; 25th and 75th centiles) are shown with white (Observer A, first measurement), light gray (Observer A, second measurement) and dark gray bars (Observer B). (CC corpus callosum, IC internal capsule, CR corona radiata, OR optic radiation, and COLL inferior colliculus.)

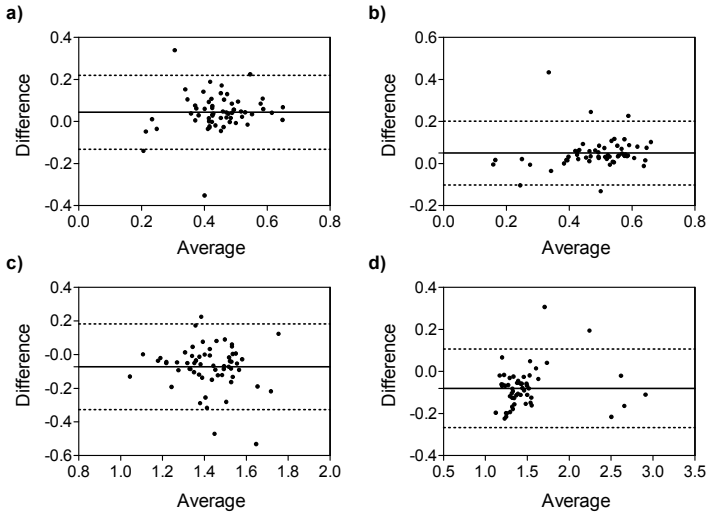

Figure 5. Bland-Altman scatter plots of the interobserver FA values in the genu (a) and splenium (b) of the corpus callosum and MD in the genu (c) and splenium (d) of the corpus callosum. The limits of agreement (dotted lines) and bias (solid line) are shown.

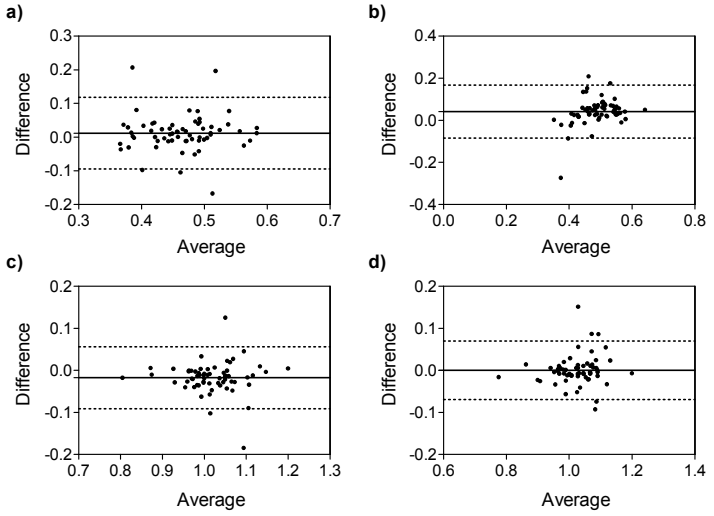

Figure 6. Bland-Altman scatter plots of the interobserver FA values in the right (a) and left (b) internal capsule and MD in the right (c) and left (d) internal capsule. The limits of agreement (dotted lines) and bias (solid line) are shown.

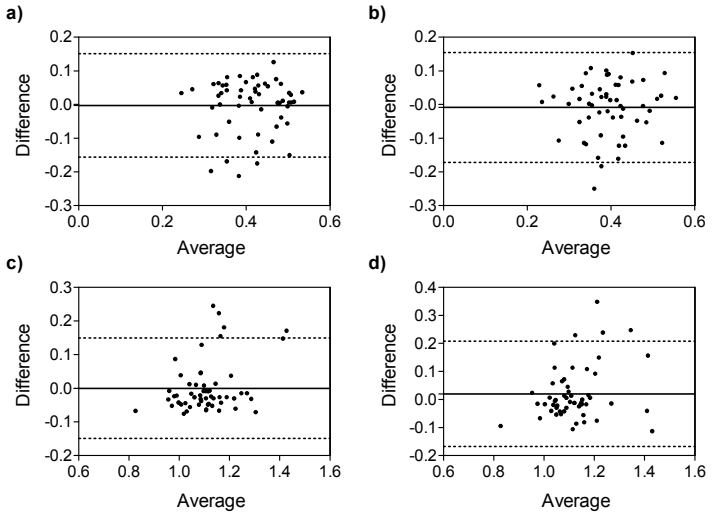

Figure 7. Bland-Altman scatter plots of the interobserver FA values in the right (a) and left (b) corona radiata and MD in the right (c) and left (d) corona radiata. The limits of agreement (dotted lines) and bias (solid line) are shown.

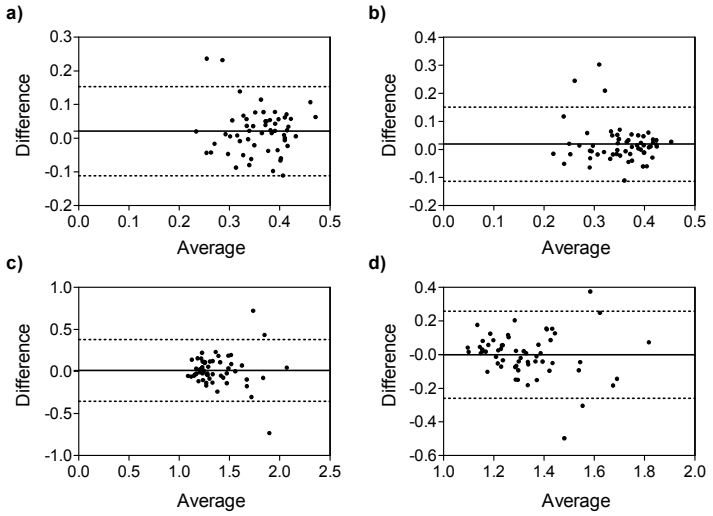

Figure 8. Bland-Altman scatter plots of the interobserver FA values in the right (a) and left (b) optic radiation and MD in the right (c) and left (d) optic radiation. The limits of agreement (dotted lines) and bias (solid line) are shown.

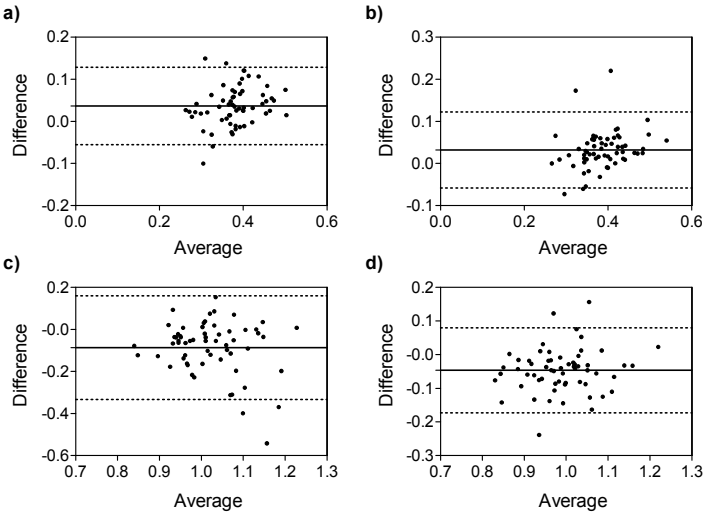

Figure 9. Bland-Altman scatter plots of the interobserver FA values in the right (a) and left (b) inferior colliculus and MD in the right (c) and left (d) inferior colliculus. The limits of agreement (dotted lines) and bias (solid line) are shown.

5.2 TBSS-ANALYSIS (STUDIES III AND IV)

5.2.1 GESTATIONAL AGE

In the TBSS analysis, no significant correlations were found between GA and FA or MD values (Study III).

5.2.2 ANTENATAL GROWTH

The AGA infants showed higher FA values (1 cluster; 27,721 voxels) in several white matter tracts at term age compared to SGA infants (Study III). Significant differences were observed in the anterior thalamic radiation, corticospinal tract, forceps major, forceps minor, inferior fronto-occipital fasciculus, inferior longitudinal fasciculus, superior longitudinal fasciculus, uncinate fasciculus, and the superior longitudinal fasciculus (temporal part). Differences were found bilaterally. Figure 10 shows the areas with significant differences between groups.

The MD values did not show significant differences between the AGA and SGA infants.

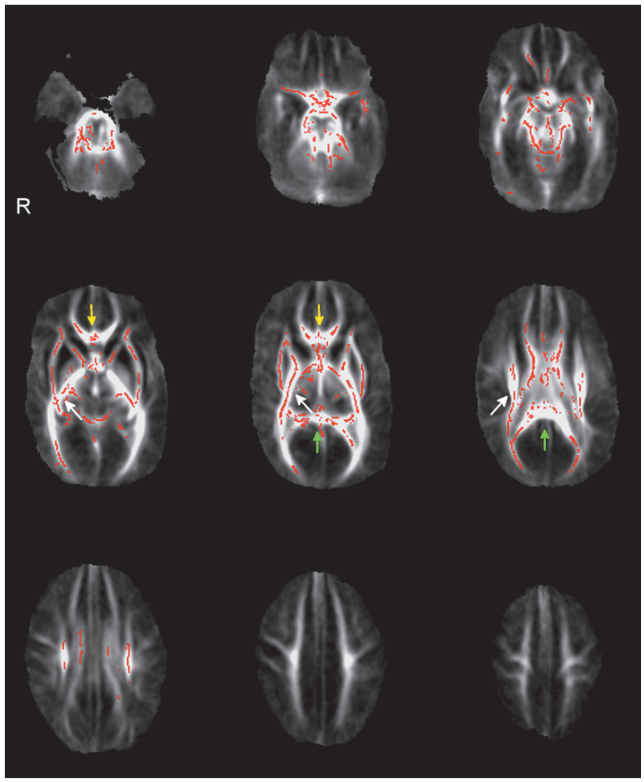

Figure 10. Appropriate-for-gestational-age (AGA) infants showed higher fractional anisotropy (FA) values than small-for-gestational-age (SGA) infants in several brain areas. Areas with a significant difference ($P<0.05$) between groups are shown in red. Three main white matter tracts are shown with arrows: the forceps major (green arrow), forceps minor (yellow arrow), and right corticospinal tract (white arrow)

5.2.3 POSTNATAL GROWTH

In the TBSS analysis (Study IV), a significant negative association ($p < 0.05$) was observed between the z-score change rate of HC and the FA values (1 cluster; 29,292 voxels). A significant positive association ($p < 0.05$) was observed between rapid postnatal growth of HC and the MD values (1 cluster; 25,760 voxels), AD values (9 clusters; 3,513, 1,616, 831, 395, 242, 109, 66, 18, 1 voxels, respectively), and RD values (1 cluster; 28,733 voxels).

Significant negative associations were found between the FA value, and significant positive associations between the MD, AD, and RD values and the z-score change rate of HC in the forceps major, forceps minor and bilaterally in the anterior thalamic radiation, corticospinal tract, cingulum (cingulate gyrus), cingulum (hippocampus), inferior fronto-occipital fasciculus, inferior longitudinal fasciculus, uncinate fasciculus, and superior longitudinal fasciculus (temporal part). The FA also showed negative associations, and MD, and RD showed also significant positive association with the z-score change rate of HC in the superior longitudinal fasciculus. The areas are shown in Figures 11, 12, 13, and 14.

No significant associations were observed between the z-score change rates of weight or length and the FA, MD, AD or RD values.

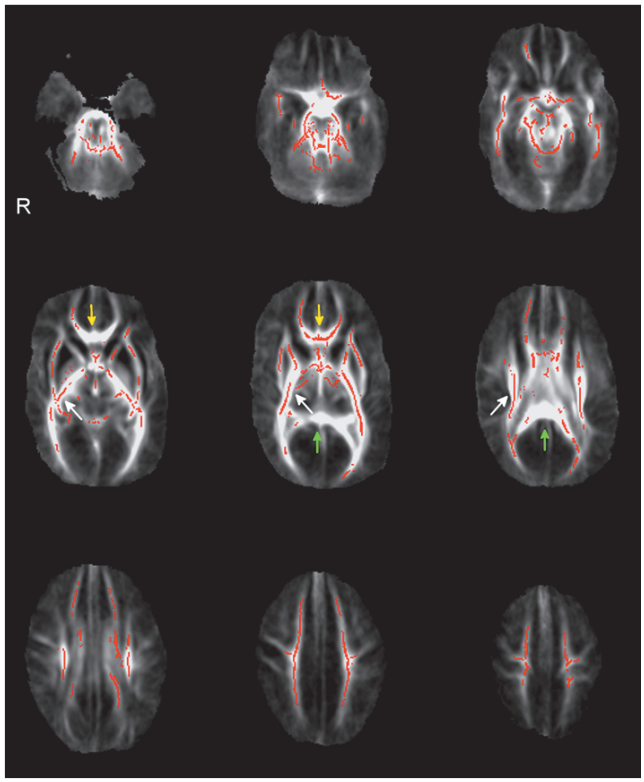

Figure 11. FA and HCs catch-up growth. A negative association was found between HCs catch-up growth and FA. Areas with significant difference ($p<0.05$) between groups are shown in red. Three main white matter tracts are shown with arrows: the forceps major (green arrow), forceps minor (yellow arrow), and right corticospinal tract (white arrow).

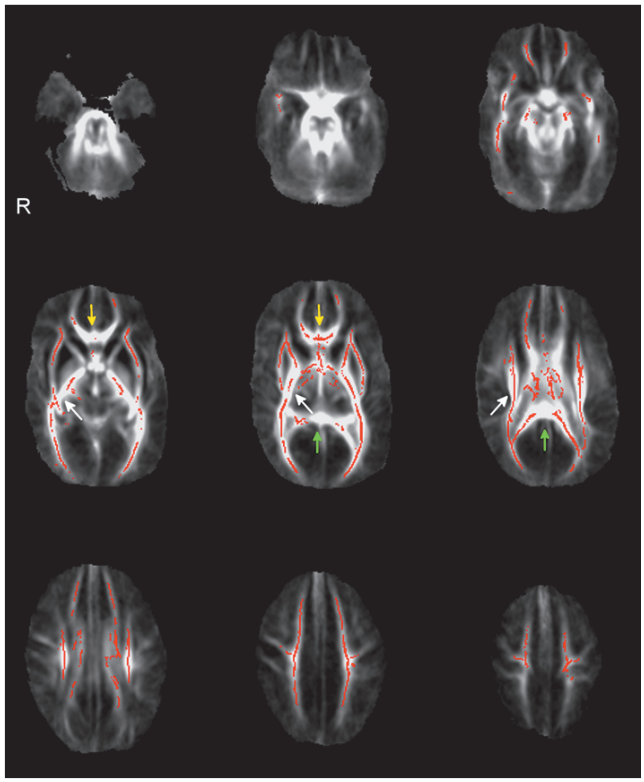

Figure 12. MD and HCs catch-up growth. A positive association was found between HCs catch-up growth and MD. Areas with significant difference ($p<0.05$) between groups are shown in red. Three main white matter tracts are shown with arrows: the forceps major (green arrow), forceps minor (yellow arrow), and right corticospinal tract (white arrow).

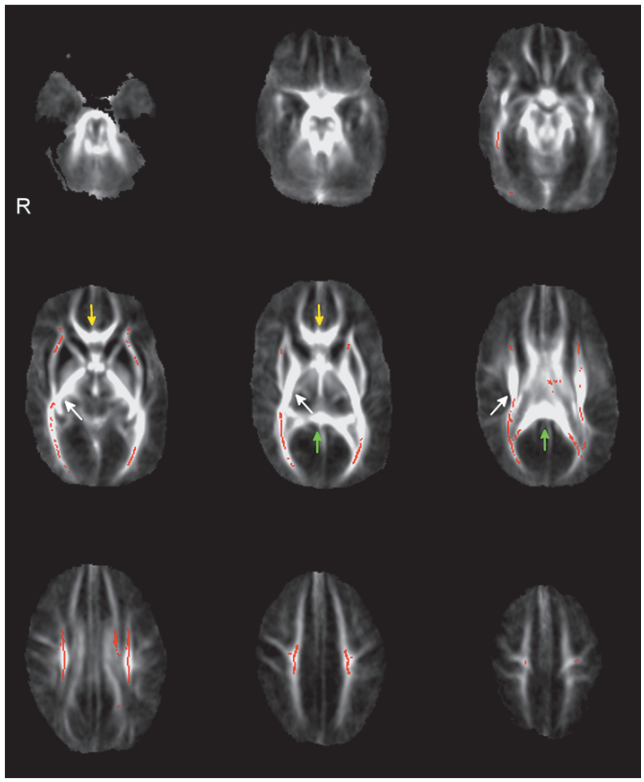

Figure 13. AD and HCs catch-up growth. A positive association was found between HCs catch-up growth and AD. Areas with significant difference ($p<0.05$) between groups are shown in red. Three main white matter tracts are shown with arrows: the forceps major (green arrow), forceps minor (yellow arrow), and right corticospinal tract (white arrow).

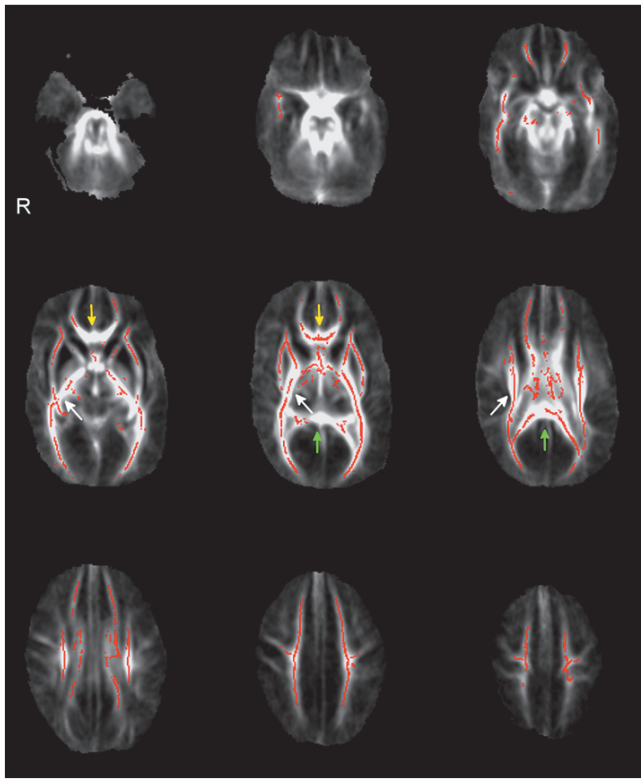

Figure 14. RD and HCs catch-up growth. A positive association was found between HCs catch-up growth and RD. Areas with significant difference ($p<0.05$) between groups are shown in red. Three main white matter tracts are shown with arrows: the forceps major (green arrow), forceps minor (yellow arrow), and right corticospinal tract (white arrow)

6 DISCUSSION

6.1 REPRODUCIBILITY OF ROI MEASUREMENTS

The ROI analysis of FA and MD in different brain areas are quite reproducible at term age, when ROI selection is undertaken using prior anatomical knowledge and variation in the ROI size is taken into account in the analysis (Study I).

The reproducibility varies between brain structures and diffusion parameters FA and MD (Study I). The variability of reproducibility reflects the fact that certain brain areas can be precisely anatomically delineated. In these areas, measurements can be performed repeatedly. In some areas, measurements can be challenging, as the reproducibility is low. This can be caused, for example, by the small size of the structure or the vicinity of ventricles.

The intraobserver reproducibility of MD values is generally better than that of FA values when assessed using ICC (Study I). Interobserver reproducibility was similar for both parameters; reproducibility was fair to good in most of the structures when assessed with ICC. However, the interobserver reproducibility was poor on the right side in the inferior colliculus for MD. The poor reproducibility values may reflect image quality issues especially PVE. The pulsatile brain motion can artificially increase MD values or increase standard deviation in structures adjacent to ventricles and inferior to the corpus callosum (Brockstedt et al. 1999, Nunes et al. 2005, Skare et al. 2001). Also differences in ROI shape or positioning in reference to white and gray matter might impact the diffusion values. These technical limitations could cause spatial heterogeneity between voxels in this structure. However, it is unclear why the effect is not bilateral.

Contradictory reproducibility results of brain FA, MD and eigenvalue measurements have been reported in adults (Bonekamp et al. 2007, Brander et al. 2010, Muller et al. 2006, Ozturk et al. 2008). Muller et al. reported high reproducibility values in the hippocampal area (Muller et al. 2006). Compared to our results, higher intraobserver reproducibility of FA and MD values (CV ≤ 2.7 % and ICC ≥ 0.96) and interobserver reproducibility (CV ≤ 2.7 % and ICC ≥ 0.90) were reported in the cerebral peduncle, anterior and posterior limb of the internal capsule, genu of corpus callosum, superior corona radiate and cingulum (Bonekamp et al. 2007). Similar regional distribution to ours was observed in a previous study in the corpus callosum, cortical spinal tract, internal capsules, basal ganglia and centrum semiovale (Ozturk et al. 2008). Comparing the limits of agreement to those published earlier, our results were similar for the capsula interna, but variation was larger in the corpus callosum as reported earlier in adults (Brander et al. 2010).

Comparing reproducibility measurement is challenging as image acquisition parameters vary between studies. Acquisition parameters that have an effect on

image quality (for example trough SNR and PVE) varied between studies (Bonekamp et al. 2007, Brander et al. 2010, Muller et al. 2006, Ozturk et al. 2008). These acquisition parameters include for example field strength, b-value, in plain resolution and slice thickness. Based on acquisition parameters, no specific reason for variation in reproducibility between studies could be concluded.

The data processing strategies vary between studies as well. Ozturk et al. performed registration between diffusion weighted images and applied the corrections to diffusion gradient directions prior to tensor fitting (Ozturk et al. 2008). The other studies do not describe the preprocessing steps. None of the studies mention if eddy current corrections were performed. This might have artefactually reduced or increased the signal intensity and also the diffusion parameters might be biased (Jones et al. 2013). All the mentioned studies used anatomical knowledge in ROI selections. However, in the study of Brander et al. 2010 the raters agreed on image levels for the measurements beforehand (Brander et al. 2010). In the study by Bonekamp et al., voxels with image intensity in the range of CSF on the b-value 0 s/mm^2 image and voxels with FA values lower than 0.2 were excluded (gray matter voxels) (Bonekamp et al. 2007). These preliminary steps in the data processing were sure to improve reproducibility.

6.2 GESTATIONAL AGE AT BIRTH

The results of this study suggest that gestational age at birth has no significant association with white matter maturation at term-equivalent age measured with FA, nor MD (Study II and Study III).

Our results are in line with those published by Bonifacio et al. and de Bruine et al., who demonstrated that white matter maturation at term age is independent of premature birth (Bonifacio et al. 2010, de Bruine et al. 2011). The previous results regarding white matter maturation are somewhat conflicting. Some previous studies have shown that prematurity affects white matter maturation at term age, for example in the posterior limb of the internal capsule and corpus callosum (Anjari et al. 2007, Hasegawa et al. 2011, Huppi et al. 1998, Thompson et al. 2011). Furthermore, in a recent work, Rose et al. reported that full-term controls showed decreased FA values compared to infants born at an earlier gestational age; for example, in the genu of the corpus callosum (Rose et al. 2008).

6.3 ANTENATAL GROWTH

The impact of antenatal growth on white matter maturation was assessed using both the ROI method (Study II) and TBSS (Study III). White matter maturation was assessed using FA and MD.

The results showed that low birth weight relative to gestational weeks is significantly associated with maturation of the corpus callosum at term age (Study II), using the ROI method. Using TBSS, it was shown that infants with impaired antenatal growth have impaired white matter maturation in several areas of the brain compared to infants with normal antenatal growth (Study III). Lower FA values were found in SGA infants than in AGA infants when GA was used as a confounding covariate in the TBSS analysis. No significant difference was observed for MD values between the study groups (Study III).

Our findings are in line with those reported earlier. In a previous study, Sanz-Cortes et al. showed that SGA children have delayed white matter maturation at gestational age 37 weeks in the pyramidal tract compared to AGA children (Sanz-Cortes et al. 2010).

The TBSS analysis showed delays in white matter maturation in several additional white matter areas compared to the ROI method (Study II and Study III). This is not particularly surprising, considering that the ROI analysis is limited to certain parts of the white matter tracts, whereas the TBSS analysis covers the whole brain. The partial volume effect caused by the positioning and size of the manually placed ROI on the tracts could also have masked the difference in white matter tracts between the AGA and SGA infants in the ROI analysis.

In the ROI analysis, MD values correlated negatively with antenatal growth in the splenium of the corpus callosum (Study II). In the TBSS, a non-significant difference was found between AGA and SGA for MD values (Study III). It is unclear why MD showed a non-significant difference between groups in TBSS and a significant difference in the ROI analysis. One possible explanation is that ROI based analyses are more sensitive than TBSS analyses to non-local and diffuse changes in the brain maturation process.

6.4 POSTNATAL GROWTH

It was shown that better head growth was associated negatively with fractional anisotropy, and positively with mean diffusivity, axial diffusivity and radial diffusivity values in several white matter areas of the brain at term age (Study IV). This indicates less mature white matter, as typical white matter maturation exhibits an increasing FA value (Aeby et al. 2009) and decreasing mean diffusivity value (Partridge et al. 2004). This finding was unexpected, as previous evidence had supported the benefits of good catch-up growth on neurodevelopment (Belfort et al. 2011, Ehrenkranz et al. 2006, Franz et al. 2009, Lundgren et al. 2008).

The results also showed that the changes were more widespread in fractional anisotropy, mean diffusivity and radial diffusivity compared to axial diffusivity. This is not completely unexpected, because in previous studies, an increase in FA values has been mainly associated with changes in radial diffusivity (Partridge et al. 2004, Suzuki et al. 2003, Thompson et al. 2011).

To understand this finding we divided the infants into two groups based on their growth pattern between birth and term age: rapid postnatal growth (positive z-score change) and slow postnatal growth (negative z-score change) of head circumference (Study IV). The infants with rapid postnatal head circumference growth were smaller at birth compared to those infants with slow postnatal growth, and 24% of those with rapid head circumference growth were small for gestational age (Study IV, Table 2).

The results suggest that rapid postnatal growth did not fully compensate for delayed brain growth and maturation in small for gestational age infants by term age (Study IV). It is possible that the catch-up growth in white matter maturation is delayed compared to catch-up growth in weight, length, and particularly head circumference. In this case, the possible positive effect might be seen at a later age. The compensation may also be only partial, as preterm infants have exhibited delayed brain maturation compared with term born controls (Huppi et al. 1998) that persists to adolescence (Constable et al. 2008) (Nagy et al. 2003).

Similar results concerning SGA birth and catch-up growth compared to brain growth have been reported earlier. De Bie et al. showed that bodily catch-up growth in children born small for gestational age does not implicate full catch-up growth of the brain at age four to seven (De Bie et al. 2011). We have found a similar effect in preterm infants at term age.

6.5 POTENTIAL LIMITATIONS

Infants born in early gestational weeks are known to have significantly more brain pathologies than infants at term age. In order to provide a more accurate picture of the preterm infant population, infants with major brain abnormalities should have been included. The infants with major brain pathologies were excluded from Studies III and IV. This was because severe brain pathologies are likely to cause local brain damage of the injured area that usually included white matter. This would have caused bias to our results, because we wanted to examine only the effect of growth on diffusion parameters in macroscopically non-damaged brains of preterm infants. In addition, severe brain pathology adds risk for growth failure. Comparison to healthy, term born controls would have further increased our understanding of the brain maturation processes.

Both analysis techniques, ROI and TBSS, would have benefitted from thinner slices. In addition, especially for TBSS, the gap between slices might have had an impact on the results. In addition, patient movement and pulsatile brain motion might have increased variation in the measured parameter values. All of this together could cause greater variation in the measured FA and MD values (Studies I and II) and therefore lower reproducibility of the ROI measurements.

In Study III, it was not possible to separate constitutionally small SGA infants from IUGR infants. This should be done in the future, as constitutionally small infants might confound the results.

Our findings on early postnatal growth might need a longer follow-up time. It would be interesting to examine multiple time points in order to see the white matter maturation pattern and to check for white matter maturation catch-up growth similar to clinical catch-up growth.

6.6 FUTURE PROSPECTS

Diffusion tensor imaging offers a new approach to study the structure and maturation of white matter. Both the ROI and TBSS analysis methods were successfully used in preterm infants. In future studies infants with major brain pathologies should also be included in the analysis.

We showed that there is a difference in the white matter maturation stage at term age between SGA and AGA infants. Restricted intrauterine growth may be a major factor affecting later brain maturation and development. The birth weight z-score should be taken into account in forthcoming studies. This finding is supported by earlier reports that associate SGA status with abnormal neurodevelopmental performance in childhood (Eixarch et al. 2008, Figueras et al. 2008, Leitner et al. 2007, Lind et al. 2011).

One challenge for future studies is to associate DTI findings with the clinical outcome of preterm infants. Quantitative diffusion tensor tractography can perhaps be used to discover associations between white matter microstructure and clinical outcomes.

7 CONCLUSION

The following conclusions can be drawn based on the results of this thesis:

Study I

The reproducibility of anatomy-based ROI measurements of brain white matter FA and MD values of preterm infants at term age was fair to good in most studied white matter structures. The visual review of the Bland-Altman scatter plots showed no considerable bias and variance was independent of the mean value. The ROI size had a significant effect on results.

Study II

Normal antenatal growth of preterm infants was associated with more mature brain white matter compared to impaired antenatal growth at term age. Gestational age at birth had no significant association with white matter maturation at term age.

Study III

AGA infants showed more mature brain white matter compared to SGA infants at term age. Gestational age at birth had no significant association with white matter maturation at term age.

Study IV

Better head growth was negatively associated with white matter maturation at term age. The results suggest that rapid postnatal growth did not fully compensate for delayed brain growth and maturation in small for gestational age infants by term age.

8 ACKNOWLEDGEMENTS

Both of my supervisors, Professor Riitta Parkkola and Dr. Markku Komu, deserve special thanks for helping me during these years. Dear Riitta: thank you for your support and encouragement. You have inspired me with your endless passion for science. 'Thanks' is a small word – but it is the best I can think of. Markku: you were my first contact with the wonderful world of magnetic resonance imaging. It has been a privilege to work with you.

I wish to express my gratitude to the official reviewers of this thesis, Docent Outi Sipilä and Docent Leena Valanne, for your constructive comments and valuable feedback.

I would like to thank my supervisory board members, Professor Pekka Hänninen and Docent Kimmo Mattila, for your guidance and advice.

I am extremely grateful to the principal investigators of the PIPARI study group: Professor Liisa Lehtonen, Professor Leena Haataja and Docent Helena Lapinleimu: you have always found time to go through data and manuscripts in addition to your other duties. I thank Professor Päivi Rautava for your suggestions and advice regarding the fourth article.

I owe my sincere gratitude to my co-authors, Dr. Teemu Paavilainen and Marika Leppänen. It has been an honor to work with you. To the two statisticians, Jaakko Matomäki and Saija Hurme, I am humbly grateful. From you I asked impossible things and I received the answers in a timely manner. These analyses would never have been done without you.

I would like to express my gratitude to all of the personnel at the Turku PET Center and Medical Imaging Center of Southwest Finland, especially Professor Juhani Knuuti, the director of the Turku PET Center, Professor Jaakko Hartiala, and Professor Pirjo Nuutila for providing such excellent research facilities. I would like to offer my deepest gratitude to all of the radiographers, laboratory technicians, doctors, and researchers. It has been enjoyable and inspiring to work with you!

I thank all my former and present physicist colleagues at Turku University Hospital, especially Mika Teräs, Tuula Tolvanen and Jarmo Teuho. You have covered for me when I have been focused on my research projects.

I want to express my gratitude to my parents, Ari and Ritva, and my brother, Matti. Thank you for the valuable discussions and support and your constant belief in me.

My warm thanks go to my dear friends.

Jani, my dear husband: your love is the light of my life. Without your encouragement, this thesis would still be just a dream.

This study was financially supported by the Emil Aaltonen Foundation, the Magnus Ehrnrooth Foundation and Turku University Hospital.

Turku, December 2013

Virva Saunavaara

9 REFERENCES

Aeby A, Liu Y, De Tiege X, Denolin V, David P, Baleriaux D, Kavec M, Metens T, and Van Bogaert P. Maturation of thalamic radiations between 34 and 41 weeks' gestation: A combined voxel-based study and probabilistic tractography with diffusion tensor imaging. American Journal of Neuroradiology. 2009;30(9):1780-1786

Ajayi-Obe M, Saeed N, Cowan FM, Rutherford MA, and Edwards AD. Reduced development of cerebral cortex in extremely preterm infants. Lancet. 2000;356(9236):1162-1163

Andersson JLR, Jenkinson M, and Smith S. Non-linear optimisation. FMRIB Analysis Group Technical Report TR07JA1. http://www.fmrib.ox.ac.uk/analysis/techrep.

Andersson JLR, Jenkinson M, and Smith S. Non-linear registration, aka Spatial normalisation. FMRIB Analysis Group Technical Report TR07JA2. http://www.fmrib.ox.ac.uk/ analysis/techrep.

Anjari M, Srinivasan L, Allsop JM, Hajnal JV, Rutherford MA, Edwards AD, and Counsell SJ. Diffusion tensor imaging with tract-based spatial statistics reveals local white matter abnormalities in preterm infants. Neuroimage. 2007;35(3):1021-1027

Arzoumanian Y, Mirmiran M, Barnes PD, Woolley K, Ariagno RL, Moseley ME, Fleisher BE, and Atlas SW. Diffusion tensor brain imaging findings at term-equivalent age may predict neurologic abnormalities in low birth weight preterm infants. American Journal of Neuroradiology. 2003;24(8):1646-1653

Ashburner J and Friston KJ. Why voxel-based morphometry should be used. Neuroimage. 2001;14(6):1238-1243

Ball G, Counsell SJ, Anjari M, Merchant N, Arichi T, Doria V, Rutherford MA, Edwards AD, Rueckert D, and Boardman JP. An optimised tract-based spatial statistics protocol for neonates: Applications to prematurity and chronic lung disease. Neuroimage. 2010;53(1):94-102

Ballabh P. Intraventricular hemorrhage in premature infants: mechanism of disease. Pediatric Research. 2010;67(1):1-8

Bammer R, Auer M, Keeling SL, Augustin M, Stables LA, Prokesch RW, Stollberger R, Moseley ME, and Fazekas F. Diffusion tensor imaging using single-shot SENSE-EPI. Magnetic Resonance in Medicine. 2002;48(1):128-136

Barkovich AJ, Kjos BO, Jackson DE, and Norman D. Normal maturation of the neonatal and infant brain - MR Imaging at 1.5 T. Radiology. 1988;166(1):173-180

Barkovich, A. James Pediatric Neuroimaging Lippincott Williams & Wilkins 2000

Basser PJ, Mattiello J, and Lebihan D. Estimation of the effective self-diffusion tensor from the NMR spin-echo. Journal of Magnetic Resonance Series B. 1994a;103(3):247-254

Basser PJ, Mattiello J, and Lebihan D. MR diffusion tensor spectroscopy and imaging. Biophysical Journal. 1994b;66(1):259-267

Basser PJ and Pajevic S. Statistical artifacts in diffusion tensor MRI (DT-MRI) caused by background noise. Magnetic Resonance in Medicine. 2000a;44(1):41-50

Basser PJ, Pajevic S, Pierpaoli C, Duda J, and Aldroubi A. In vivo fiber tractography using DT-MRI data. Magnetic Resonance in Medicine. 2000b;44(4):625-632

Basser PJ and Pierpaoli C. Microstructural and physiological features of tissues elucidated by quantitative-diffusion-tensor MRI. Journal of Magnetic Resonance Series B. 1996;111(3):209-219

Beaulieu C. The basis of anisotropic water diffusion in the nervous system - a technical review. Nmr in Biomedicine. 2002;15(7-8):435-455

Behrens TEJ, Berg HJ, Jbabdi S, Rushworth MFS, and Woolrich MW. Probabilistic diffusion tractography with multiple fibre orientations: What can we gain? Neuroimage. 2007;34(1):144-155

Behrman, Richard E Preterm Birth: Causes, Consequences, and Prevention National Academies Press (US) 2007

Belfort MB, Rifas-Shiman SL, Sullivan T, Collins CT, Mcphee AJ, Ryan P, Kleinman KP, Gillman MW, Gibson RA, and Makrides M. Infant growth before and after term: Effects on neurodevelopment in preterm infants. Pediatrics. 2011;128(4):E899-E906

Berman JI, Glass HC, Miller SP, Mukherjee P, Ferriero DM, Barkovich AJ, Vigneron DB, and Henry RG. Quantitative fiber tracking analysis of the optic radiation correlated with visual performance in premature newborns. American Journal of Neuroradiology. 2009;30(1):120-124

Berman JI, Mukherjee P, Partridge SC, Miller SP, Ferriero DM, Barkovich AJ, Vigneron DB, and Henry RG. Quantitative diffusion tensor MRI fiber tractography of sensorimotor white matter development in premature infants. Neuroimage. 2005;27(4):862-871

Bernstein, Matt A., King, Kevin F., and Zhou, Xiaohong J Handbook of MRI Pulse Sequences Academic Press 2004

Bland JM and Altman DG. Statistical-methods for assessing agreement between 2 methods of clinical measurement. Lancet. 1986;1(8476):307-310

Bloch F. Nuclear induction. Physical Review. 1946;70(7-8):460-474

Bonekamp D, Nagae LM, Degaonkar M, Matson M, Abdalla WMA, Barker PB, Mori S, and Horska A. Diffusion tensor imaging in children and adolescents: Reproducibility, hemispheric, and age-related differences. Neuroimage. 2007;34(2):733-742

Bonifacio SL, Glass HC, Chau V, Berman JI, Xu DA, Brant R, Barkovich AJ, Poskitt KJ, Miller SP, and Ferriero DM. Extreme premature birth is not associated with impaired development of brain microstructure. Journal of Pediatrics. 2010;157(5):726-U55

Bookstein FL. "Voxel-based morphometry" should not be used with imperfectly registered images. Neuroimage. 2001;14(6):1454-1462

Boujraf S, Luypaert R, Shabana W, De Meirleir L, Sourbron S, and Osteaux M. Study of pediatric brain development using magnetic resonance imaging of anisotropic diffusion. Magnetic Resonance Imaging. 2002;20(4):327-336

Brander A, Kataja A, Saastamoinen A, Ryymin P, Huhtala H, hman J, Soimakallio S, and Dastidar P. Diffusion tensor imaging of the brain in a healthy adult population: Normative values and measurement reproducibility at 3 T and 1.5 T. Acta Radiologica. 2010;51(7):800-807

Brockstedt S, Borg M, Geijer B, Wirestam R, Thomsen C, Holtas S, and Stahlberg F. Triggering in quantitative diffusion imaging with single-shot EPI. Acta Radiologica. 1999;40(3):263-269

Brody BA, Kinney HC, Kloman AS, and Gilles FH. Sequence of central-nervous-system myelination in human Infancy .1. An autopsy study of myelination. Journal of Neuropathology and Experimental Neurology. 1987;46(3):283-301

Brown R. A brief account of microscopical observations in the months June, July and August 1827 on the particles contained in pollen. Edinburgh New Philosophical Journal. 1827;5:358-371

Chiswick ML. Commentary on current World-Health-Organization definitions used in perinatal statistics. British Journal of Obstetrics and Gynaecology. 1986;93(12):1236-1238

Chung SW, Pelletier D, Sdika M, Lu Y, Berman JL, and Henry RG. Whole brain voxel-wise analysis of single-subject serial DTI by permutation testing. Neuroimage. 2008;39(4):1693-1705

Constable RT, Ment LR, Vohr BR, Kesler SR, Fulbright RK, Lacadie C, Delancy S, Katz KH, Schneider KC, Schafer RJ, Makuch RW, and Reiss AR. Prematurely born children demonstrate white matter microstructural differences at 12 years of age, relative to term control subjects: An investigation of group and gender effects. Pediatrics. 2008;121(2):306-316

Conturo TE, Lori NF, Cull TS, Akbudak E, Snyder AZ, Shimony JS, McKinstry RC, Burton H, and Raichle ME. Tracking neuronal fiber pathways in the living human brain. Proceedings of the National Academy of Sciences of the United States of America. 1999;96(18):10422-10427

Counsell SJ, Shen YJ, Boardman JP, Larkman DJ, Kapellou O, Ward P, Allsop JM, Cowan FM, Hajnal JV, Edwards AD, and Rutherford MA. Axial and radial diffusivity in preterm infants who have diffuse white matter changes on magnetic resonance imaging at term-equivalent age. Pediatrics. 2006;117(2):376-386

Damadian R. Tumor detection by Nuclear Magnetic Resonance. Science. 1971;171(3976):1151

De Bie HMA, Oostrom KJ, Boersma M, Veltman DJ, Barkhof F, Delemarre-van de Waal HA, and van den Heuvel MP. Global and regional differences in brain anatomy of young children born small for gestational age. PLoS ONE. 2011;6(9)

de Bruine FT, van Wezel-Meijler G, Leijser LM, Berg-Huysmans AA, van Steenis A, van Buchem MA, and van der Grond J. Tractography of developing white matter of the internal capsule and corpus callosum in very preterm infants. European Radiology. 2011;21(3):538-547

Dixon RL and Ekstrand KE. The physics of proton NMR. Medical Physics. 1982;9(6):807-818

Drobyshevsky A, Bregman J, Storey P, Meyer J, Prasad PV, Derrick M, MacKendrick W, and Tan S. Serial diffusion tensor imaging detects white matter changes that correlate with motor outcome in premature infants. Developmental Neuroscience. 2007;29(4-5):289-301

Dubois J, Dehaene-Lambertz G, Perrin M, Mangin JF, Cointepas Y, Duchesnay E, Le Bihan D, and Hertz-Pannier L. Asynchrony of the early maturation of white matter bundles in healthy infants: Quantitative landmarks revealed noninvasively by diffusion tensor imaging. Human Brain Mapping. 2008a;29(1):14-27

Dubois J, Dehaene-Lambertz G, Soares C, Cointepas Y, Le Bihan D, and Hertz-Pannier L. Microstructural correlates of infant functional development: Example of the visual pathways. Journal of Neuroscience. 2008b;28(8):1943-1948

Dubois J, Hertz-Pannier L, Cachia A, Mangin JF, Le Bihan D, and Dehaene-Lambertz G. Structural asymmetries in the infant language and sensori-motor networks. Cerebral Cortex. 2009;19(2):414-423

Dubois J, Hertz-Pannier L, Dehaene-Lambertz G, Cointepas Y, and Le Bihan D. Assessment of the early organization and maturation of infants' cerebral white matter fiber bundles: A feasibility study using quantitative diffusion tensor imaging and tractography. Neuroimage. 2006;30(4):1121-1132

Dudink J, Lequin M, van Pul C, Buijs J, Conneman N, van Goudoever J, and Govaert P. Fractional anisotropy in white matter tracts of very-low-birth-weight infants. Pediatric Radiology. 2007;37(12):1216-1223

Ebisu T, Naruse S, Horikawa Y, Ueda S, Tanaka C, Uto M, Umeda M, and Higuchi T. Discrimination between different types of white-matter edema with diffusion-weighted MR-Imaging. Journal of Magnetic Resonance Imaging. 1993;3(6):863-868

Ehrenkranz RA, Dusick AM, Vohr BR, Wright LL, Wrage LA, and Poole WK. Growth in the neonatal intensive care unit influences neurodevelopmental and growth outcomes of extremely low birth weight infants. Pediatrics. 2006;117(4):1253-1261

Eixarch E, Batalle D, Illa M, Munoz-Moreno E, Arbat-Plana A, Amat-Roldan I, Figueras F, and Gratacos E. Neonatal neurobehavior and diffusion MRI changes in brain reorganization due to intrauterine growth restriction in a rabbit model. PLoS ONE. 2012;7(2)

Eixarch E, Meler E, Iraola A, Illa M, Crispi F, Hernandez-Andrade E, Gratacos E, and Figueras F. Neurodevelopmental outcome in 2-year-old infants who were small-for-gestational age term fetuses with cerebral blood flow redistribution. Ultrasound in Obstetrics & Gynecology. 2008;32(7):894-899

Euser AM, de Wit CC, Finken MJJ, Rijken M, and Wit JM. Growth of preterm born children. Hormone Research. 2008;70(6):319-328

Figueras F, Eixarch E, Gratacos E, and Gardosi J. Predictiveness of antenatal umbilical artery Doppler for adverse pregnancy outcome in small-for-gestational-age babies according to customised birthweight centiles: population-based study. Bjog-An International Journal of Obstetrics and Gynaecology. 2008;115(5):590-594

Fleiss, Joseph L. The Design and Analysis of Clinical Experiments Wiley 1986

Frackowiak, R. S. J., Friston, K. J., Frith, C. D., Dolan, J., and azziotta, J. C. Human Brain Function Academic Press USA 1997

Franz AR, Pohlandt F, Bode H, Mihatsch WA, Sander S, Kron M, and Steinmacher J. Intrauterine, Early Neonatal, and Postdischarge Growth and Neurodevelopmental Outcome at 5.4 Years in Extremely Preterm Infants After Intensive Neonatal Nutritional Support. Pediatrics. 2009;123(1):E101-E109

Frisk V, Amsel R, and Whyte HEA. The importance of head growth patterns in predicting the cognitive abilities and literacy skills of small-for-gestational-age children. Developmental Neuropsychology. 2002;22(3):565-593

Garroway AN, Grannell PK, and Mansfield P. Image-formation in NMR by a selective irradiative process. Journal of Physics C-Solid State Physics. 1974;7(24):L457-L462

Gimenez M, Miranda MJ, Born AP, Nagy Z, Rostrup E, and Jernigan TL. Accelerated cerebral white matter development in preterm infants: A voxel-based morphometry study with diffusion tensor MR imaging. Neuroimage. 2008;41(3):728-734

Hahn EL. Spin Echoes. Physical Review. 1950;80(4):580-594

Hasegawa T, Yamada K, Morimoto M, Morioka S, Tozawa T, Isoda K, Murakami A, Chiyonobu T, Tokuda S, Nishimura A, Nishimura T, and Hosoi H. Development of corpus callosum in preterm infants is affected by the prematurity: in vivo assessment of diffusion tensor imaging at term-equivalent age. Pediatric Research. 2011;69(3):249-254

Hermoye L, Saint-Maitin C, Cosnard G, Lee SK, Kim J, Nassogne MC, Menten R, Clapuyt P, Donohue PK, Hua KG, Wakana S, Jiang HY, van Zijl PCM, and Mori S. Pediatric diffusion tensor imaging: Normal database and observation of the white matter maturation in early childhood. Neuroimage. 2006;29(2):493-504

Huppi PS, Maier SE, Peled S, Zientara GP, Barnes PD, Jolesz FA, and Volpe JJ. Microstructural development of human newborn cerebral white matter assessed in vivo by diffusion tensor magnetic resonance imaging. Pediatric Research. 1998;44(4):584-590

Huppi PS, Zimine S, Borradori-Tolsa C, Lodygenski G, and Lazeyras F. Microstructural changes in brain development in premature infants with intrauterine growth restriction (IUGR): A voxel-based analysis of diffusion tensor imaging (DTI). Pediatric Research. 2004;55(4):582A-582A

Inder TE, Warfield SK, Wang H, Huppi PS, and Volpe JJ. Abnormal cerebral structure is present at term in premature infants. Pediatrics. 2005;115(2):286-294

Jeurissen B, Leemans A, Tournier JD, Jones DK, and Sijbers J. Investigating the prevalence of complex fiber configurations in white matter tissue with diffusion magnetic resonance imaging. Hum.Brain Mapp. 2012

Jones DK, Knosche TR, and Turner R. White matter integrity, fiber count, and other fallacies: The do's and don'ts of diffusion MRI. Neuroimage. 2013;73:239-254

Jones DK, Symms MR, Cercignani M, and Howard RJ. The effect of filter size on VBM analyses of DT-MRI data. Neuroimage. 2005;26(2):546-554

Jones RA, Palasis S, and Grattan-Smith JD. MRI of the neonatal brain: Optimization of spin-echo parameters. American Journal of Roentgenology. 2004;182(2):367-372

Korvenranta E, Lehtonen L, Peltola M, Hakkinen U, Andersson S, Gissler M, Hallman M, Leipala J, Rautava L, Tammela O, and Linna M. Morbidities and hospital resource use during the first 3 years of life among very preterm infants. Pediatrics. 2009;124(1):128-134

Kostovic I and Judas M. The development of the subplate and thalamocortical connections in the human foetal brain. Acta Paediatrica. 2010;99(8):1119-1127

Lancaster JL, Rainey LH, Summerlin JL, Freitas CS, Fox PT, Evans AC, Toga AW, and Mazziotta JC. Automated labeling of the human brain: A preliminary report on the development and evaluation of a forward-transform method. Human Brain Mapping. 1997;5(4):238-242

Lancaster JL, Woldorff MG, Parsons LM, Liotti M, Freitas ES, Rainey L, Kochunov PV, Nickerson D, Mikiten SA, and Fox PT. Automated Talairach Atlas labels for functional brain mapping. Human Brain Mapping. 2000;10(3):120-131

Lauterbur PC. Image formation by induced local interactions - examples employing Nuclear Magnetic-Resonance. Nature. 1973;242(5394):190-191

Lazar M and Alexander AL. Bootstrap white matter tractography (BOOT-TRAC). Neuroimage. 2005;24(2):524-532

Le Bihan D. Molecular diffusion, tissue microdynamics and microstructure. Nmr in Biomedicine. 1995;8(7-8):375-386

Le Bihan D, Mangin JF, Poupon C, Clark CA, Pappata S, Molko N, and Chabriat H. Diffusion tensor imaging: Concepts and applications. Journal of Magnetic Resonance Imaging. 2001;13(4):534-546

Le Bihan D, Poupon C, Amadon A, and Lethimonnier F. Artifacts and pitfalls in diffusion MRI. Journal of Magnetic Resonance Imaging. 2006;24(3):478-488

Lee PA, Chernausek SD, Hokken-Koelega ACS, and Czernichow P. International small for gestational age advisory board consensus development conference statement: Management of short children born small for gestational age, April 24 October 1, 2001. Pediatrics. 2003;111(6):1253-1261

Lehtonen L, Rautava L, Korvenranta E, Korvenranta H, Peltola M, and Hakkinen U. PERFECT preterm infant study. Annals of Medicine. 2011;43:S47-S53

Leijser LM, de Bruine FT, Steggerda SJ, van der Grond J, Walther FJ, and van Wezel-Meijler G. Brain imaging findings in very preterm infants throughout the neonatal period: Part I. Incidences and evolution of lesions, comparison between ultrasound and MRI. Early Human Development. 2009;85(2):101-109

Leitner Y, Fattal-Valevski A, Geva R, Eshel R, Toledano-Alhadef H, Rotstein M, Bassan H, Radianu B, Bitchonsky O, Jaffa AJ, and Harel S. Neurodevelopmental outcome of children with intrauterine growth retardation: A longitudinal, 10-year prospective study. Journal of Child Neurology. 2007;22(5):580-587

Leung C. Born too soon. Neuroendocrinology Letters. 2004;25:133-136

Levitt, Malcolm H. Spin Dynamics: Basics of Nuclear Magnetic Resonance John Wiley & Sons Ltd 2001

Lind A, Korkman M, Lehtonen L, Lapinleimu H, Parkkola R, Matomaki J, and Haataja L. Cognitive and neuropsychological outcomes at 5 years of age in preterm children born in the 2000s. Developmental Medicine and Child Neurology. 2011;53(3):256-262

Liu Y, Aeby A, Baleriaux D, David P, Absil J, De Maertelaer V, Van Bogaert P, Avni F, and Metens T. White matter abnormalities are related to microstructural changes in preterm neonates at term-equivalent age: A diffusion tensor imaging and probabilistic tractography study. American Journal of Neuroradiology. 2012;33(5):839-845

Liu Y, Baleriaux D, Kavec M, Metens T, Absil J, Denolin V, Pardou A, Avni F, Van Bogaert P, and Aeby A. Structural asymmetries in motor and language networks in a population of healthy preterm neonates at term equivalent age: A diffusion tensor imaging and probabilistic tractography study. Neuroimage. 2010;51(2):783-788

Lundgren EM, Cnattingius S, Jonsson B, and Tuvemo T. Intellectual and psychological performance in males born small for gestational age with and without catch-up growth. Pediatric Research. 2001;50(1):91-96

Lundgren EM and Tuvemo T. Effects of being born small for gestational age on long-term intellectual performance. Best Practice & Research Clinical Endocrinology & Metabolism. 2008;22(3):477-488

Lundgren M, Cnattingius S, Jonsson B, and Tuvemo T. Intellectual performance in young adult males born small for gestational age. Growth Hormone & Igf Research. 2004;14:S7-S8

Mansfield P. Multi-planar image-formation using NMR spin echoes. Journal of Physics C-Solid State Physics. 1977;10(3):L55-L58

Mansfield P and Grannell PK. NMR diffraction in solids. Journal of Physics C-Solid State Physics. 1973;6(22):L422-L426

Mansfield P and Pykett IL. Biological and medical imaging by NMR. Journal of Magnetic Resonance. 1978;29(2):355-373

Maunu J, Kirjavainen J, Korja R, Parkkola R, Rikalainen H, Lapinleimu H, Haataja L, and Lehtonen L. Relation of prematurity and brain injury to crying behavior in infancy. Pediatrics. 2006;118(1):E57-E65

Metzler-Baddeley C, O'Sullivan MJ, Bells S, Pasternak O, and Jones DK. How and how not to correct for CSF-contamination in diffusion MRI. Neuroimage. 2012;59(2):1394-1403

Miller SP, Vigneron DB, Henry RG, Bohland MA, Ceppi-Cozzio C, Hoffman C, Newton N, Partridge JC, Ferriero DM, and Barkovich AJ. Serial quantitative diffusion tensor MRI of the premature brain: Development in newborns with and without injury. Journal of Magnetic Resonance Imaging. 2002;16(6):621-632

Mori S, Crain BJ, Chacko VP, and van Zijl PCM. Three-dimensional tracking of axonal projections in the brain by magnetic resonance imaging. Annals of Neurology. 1999;45(2):265-269

Mori S and van Zijl PCM. Fiber tracking: principles and strategies - A technical review. Nmr in Biomedicine. 2002;15(7-8):468-480

Mori S and Zhang JY. Principles of diffusion tensor imaging and its applications to basic neuroscience research. Neuron. 2006;51(5):527-539

Mukherjee P, Miller JH, Shimony JS, Philip JV, Nehra D, Snyder AZ, Conturo TE, Neil JJ, and McKinstry RC. Diffusion-tensor MR imaging of gray and white matter development during normal human brain maturation. American Journal of Neuroradiology. 2002;23(9):1445-1456

Muller MJ, Mazanek M, Weibrich C, Dellani PR, Stoeter P, and Fellgiebel A. Distribution characteristics, reproducibility, and precision of region of interest-based hippocampal diffusion tensor imaging measures. American Journal of Neuroradiology. 2006;27(2):440-446

Nagy Z, Westerberg H, Skare S, Andersson JL, Lilja A, Flodmark O, Fernell E, Holmberg K, Bohm B, Forssberg H, Lagercrantz H, and Klingberg T. Preterm children have disturbances of white matter at 11 years of age as shown by diffusion tensor imaging. Pediatric Research. 2003;54(5):672-679

Neil J, Miller J, Mukherjee P, and Huppi PS. Diffusion tensor imaging of normal and injured developing human brain - A technical review. Nmr in Biomedicine. 2002;15(7-8):543-552

Neil JJ, Shiran SI, McKinstry RC, Schefft GL, Snyder AZ, Almli CR, Akbudak E, Aronovitz JA, Miller JP, Lee BCP, and Conturo TE. Normal brain in human newborns: Apparent diffusion coefficient and diffusion anisotropy measured by using diffusion tensor MR imaging. Radiology. 1998;209(1):57-66

Nichols, T. Randomise Theory. 1-5-2013. http://fsl.fmrib.ox.ac.uk/fsl/fslwiki/Randomise/Theory.

Nowell MA, Hackney DB, Zimmerman RA, Bilaniuk LT, Grossman RI, and Goldberg HI. Immature brain - Spin-Echo Pulse Sequence parameters for high-contrast MR Imaging. Radiology. 1987;162(1):272-273

Nunes RG, Jezzard P, and Clare S. Investigations on the efficiency of cardiac-gated methods for the acquisition of diffusion-weighted images. Journal of Magnetic Resonance. 2005;177(1):102-110

Ozturk A, Sasson AD, Farrell JAD, Landman BA, da Motta ACBS, Aralasmak A, and Yousem DM. Regional differences in diffusion tensor imaging measurements: Assessment of intrarater and interrater variability. American Journal of Neuroradiology. 2008;29(6):1124-1127

Pajevic S and Pierpaoli C. Color schemes to represent the orientation of anisotropic tissues from diffusion tensor data: Application to white matter fiber tract mapping in the human brain. Magnetic Resonance in Medicine. 1999;42(3):526-540

Papadakis NG, Xing D, Houston GC, Smith JM, Smith MI, James MF, Parsons AA, Huang CLH, Hall LD, and Carpenter TA. A study of rotationally invariant and symmetric indices of diffusion anisotropy. Magnetic Resonance Imaging. 1999;17(6):881-892

Parker GJM, Haroon HA, and Wheeler-Kingshott CAM. A framework for a streamline-based probabilistic index of connectivity (PICo) using a structural interpretation of MRI diffusion measurements. Journal of Magnetic Resonance Imaging. 2003;18(2):242-254

Partridge SC, Mukherjee P, Berman JI, Henry RG, Miller SP, Lu Y, Glenn OA, Ferriero DM, Barkovich AJ, and Vigneron DB. Tractography-based quantitation of diffusion tensor imaging parameters in white matter tracts of preterm newborns. Journal of Magnetic Resonance Imaging. 2005;22(4):467-474

Partridge SC, Mukherjee P, Henry RG, Miller SP, Berman JI, Jin H, Lu Y, Glenn OA, Ferriero DM, Barkovich AJ, and Vigneron DB. Diffusion tensor imaging: serial quantitation of white matter tract maturity in premature newborns. Neuroimage. 2004;22(3):1302-1314

Pierpaoli C and Basser PJ. Toward a quantitative assessment of diffusion anisotropy. Magnetic Resonance in Medicine. 1996a;36(6):893-906

Pierpaoli C, Jezzard P, Basser PJ, Barnett A, and DiChiro G. Diffusion tensor MR imaging of the human brain. Radiology. 1996b;201(3):637-648

Pihkala J, Hakala T, Voutilainen P, and Raivio K. [Characteristic of recent fetal growth curves in Finland]. Duodecim. 1989;105(18):1540-1546

Provenzale JM, Isaacson J, and Chen S. Progression of corpus callosum diffusion-tensor imaging values during a period of signal changes consistent with myelination. American Journal of Roentgenology. 2012;198(6):1403-1408

Provenzale JM, Liang L, DeLong D, and White LE. Diffusion tensor imaging assessment of brain white matter maturation during the first postnatal year. American Journal of Roentgenology. 2007;189(2):476-486

Pruessmann KP, Weiger M, Scheidegger MB, and Boesiger P. SENSE: Sensitivity encoding for fast MRI. Magnetic Resonance in Medicine. 1999;42(5):952-962

Purcell EM, Torrey HC, and Pound RV. Resonance absorption by nuclear magnetic moments in a solid. Physical Review. 1946;69(1-2):37-38

Ramenghi LA, Martinelli A, De Carli A, Brusati V, Mandia L, Fumagalli M, Triulzi F, Mosca F, and Cetin I. Cerebral maturation in IUGR and appropriate for gestational age preterm babies. Reproductive Sciences. 2011;18(5):469-475

Reese TG, Heid O, Weisskoff RM, and Wedeen VJ. Reduction of eddy-current-induced distortion in diffusion MRI using a twice-refocused spin echo. Magnetic Resonance in Medicine. 2003;49(1):177-182

Rose J, Butler EE, Lamont LE, Barnes PD, Atlas SW, and Stevenson DK. Neonatal brain structure on MRI and diffusion tensor imaging, sex, and neurodevelopment in very-low-birthweight preterm children. Developmental Medicine and Child Neurology. 2009;51(7):526-535

Rose SE, Hatziaeorgiou X, Strudwick MW, Durbridge G, Davies PSI, and Colditz PB. Altered white matter diffusion anisotropy in normal and preterm infants at term-equivalent age. Magnetic Resonance in Medicine. 2008;60(4):761-767

Saksena S, Husain N, Malik GK, Trivedi R, Sarma M, Rathore RS, Pandey CM, and Gupta RK. Comparative evaluation of the cerebral and cerebellar white matter development in pediatric age group using quantitative diffusion tensor imaging. Cerebellum. 2008;7(3):392-400

Sanz-Cortes M, Figueras F, Bargallo N, Padilla N, Amat-Roldan I, and Gratacos E. Abnormal brain microstructure and metabolism in small-for-gestational-age term fetuses with normal umbilical artery Doppler. Ultrasound in Obstetrics & Gynecology. 2010;36(2):159-165

Sie LTL, vanderKnaap MS, vanWezelMeijler G, and Valk J. MRI assessment of myelination of motor and sensory pathways in the brain of preterm and term-born infants. Neuropediatrics. 1997;28(2):97-105

Sizonenko V, Borradori-Tolsa C, Vauthay DM, Lodygensky G, Lazeyras F, and Huppi PS. Impact of intrauterine growth restriction and glucocorticoids on brain development: Insights using advanced magnetic resonance imaging. Molecular and Cellular Endocrinology. 2006;254-255(0):163-171

Skare S and Andersson JLR. On the effects of gating in diffusion imaging of the brain using single shot EPI. Magnetic Resonance Imaging. 2001;19(8):1125-1128

Skiold B, Horsch S, Hallberg B, Engstrom M, Nagy Z, Mosskin M, Blennow M, and Aden U. White matter changes in extremely preterm infants, a population-based diffusion tensor imaging study. Acta Paediatrica. 2010;99(6):842-849

Smith SM. Fast robust automated brain extraction. Human Brain Mapping. 2002;17(3):143-155

Smith SM, Jenkinson M, Johansen-Berg H, Rueckert D, Nichols TE, Mackay CE, Watkins KE, Ciccarelli O, Cader MZ, Matthews PM, and Behrens TEJ. Tract-based spatial statistics: Voxelwise analysis of multi-subject diffusion data. Neuroimage. 2006;31(4):1487-1505

Smith SM, Jenkinson M, Woolrich MW, Beckmann CF, Behrens TEJ, Johansen-Berg H, Bannister PR, De Luca M, Drobnjak I, Flitney DE, Niazy RK, Saunders J, Vickers J, Zhang YY, De Stefano N, Brady JM, and Matthews PM. Advances in functional and structural MR image analysis and implementation as FSL. Neuroimage. 2004;23:S208-S219

Smith SM and Nichols TE. Threshold-free cluster enhancement: Addressing problems of smoothing, threshold dependence and localisation in cluster inference. Neuroimage. 2009;44(1):83-98

Sorva R, Tolppanen EM, and Perheentupa J. Variation of growth in length and weight of children .1. years 1 and 2. Acta Paediatrica Scandinavica. 1990;79(5):490-497

Stehling MK, Turner R, and Mansfield P. Echo-Planar Imaging - Magnetic-Resonance-Imaging in a fraction of a second. Science. 1991;254(5028):43-50

Stejskal EO and Tanner JE. Spin diffusion measurements - spin echoes in presence of a time-dependent field gradient. Journal of Chemical Physics. 1965;42(1):288-

Stiles J and Jernigan TL. The basics of brain development. Neuropsychology Review. 2010;20(4):327-348

STUK. Magneettitutkimus. 17-5-2013. http://www.stuk.fi/sateilyn-hyodyntaminen/terveydenhuolto/fi_FI/magneetti.

Suzuki Y, Matsuzawa H, Kwee IL, and Nakada T. Absolute eigenvalue diffusion tensor analysis for human brain maturation. Nmr in Biomedicine. 2003;16(5):257-260

Tau GZ and Peterson BS. Normal development of brain circuits. Neuropsychopharmacology. 2010;35(1):147-168

Thompson DK, Inder TE, Faggian N, Johnston L, Warfield SK, Anderson PJ, Doyle LW, and Egan GF. Characterization of the corpus callosum in very preterm and full-term infants utilizing MRI. Neuroimage. 2011;55(2):479-490

Thompson DK, Warfield SK, Carlin JB, Pavlovic M, Wang HX, Bear M, Kean MJ, Doyle LW, Egan GF, and Inder TE. Perinatal risk factors altering regional brain structure in the preterm infant. Brain. 2007;130:667-677

Tuch DS, Reese TG, Wiegell MR, Makris N, Belliveau JW, and Wedeen VJ. High angular resolution diffusion imaging reveals intravoxel white matter fiber heterogeneity. Magnetic Resonance in Medicine. 2002;48(4):577-582

Tucker J and McGuire W. ABC of preterm birth - Epidemiology of preterm birth. British Medical Journal. 2004;329(7467):675-678

Tzourio-Mazoyer N, Landeau B, Papathanassiou D, Crivello F, Etard O, Delcroix N, Mazoyer B, and Joliot M. Automated anatomical labeling of activations in SPM using a macroscopic anatomical parcellation of the MNI MRI single-subject brain. Neuroimage. 2002;15(1):273-289

Van Kooij BJ, de Vries LS, Ball G, Van Haastert IC, Benders MJ, Groenendaal F, and Counsell SJ. Neonatal tract-based spatial statistics findings and outcome in preterm infants. American Journal of Neuroradiology. 2012;33(1):188-194

Volpe JJ. Brain injury in premature infants: a complex amalgam of destructive and developmental disturbances. Lancet Neurology. 2009;8(1):110-124

Vos SB, Jones DK, Viergever MA, and Leemans A. Partial volume effect as a hidden covariate in DTI analyses. Neuroimage. 2011;55(4):1566-1576

Webster, Matthew. FMRIB58_FA. 13-8-2012a. http://fsl.fmrib.ox.ac.uk/fsl/fslwiki/FMRIB58_FA.

Webster, Matthew. TBSS UserGuide. 4-9-2012b. http://fsl.fmrib.ox.ac.uk/fsl/fslwiki/TBSS.

Xue R, van Zijl PCM, Crain BJ, Solaiyappan M, and Mori S. In vivo three-dimensional reconstruction of rat brain axonal projections by diffusion tensor imaging. Magnetic Resonance in Medicine. 1999;42(6):1123-1127